POLITECNICO DI TORINO
Repository ISTITUZIONALE

Geophysical–geotechnical methodology for assessing the spatial distribution of glaciolacustrine sediments: The case history of Lake Seracchi

Original
Geophysical–geotechnical methodology for assessing the spatial distribution of glaciolacustrine sediments: The case history of Lake Seracchi / Vergnano, Andrea; Oggeri, Claudio; Godio, Alberto. - In: EARTH SURFACE PROCESSES AND LANDFORMS. - ISSN 0197-9337. - (2023), pp. 1-24. [10.1002/esp.5555]

Availability:
This version is available at: 11583/2976030 since: 2023-02-14T13:39:13Z

Publisher:
Wiley

Published
DOI:10.1002/esp.5555

Terms of use:

This article is made available under terms and conditions as specified in the corresponding bibliographic description in the repository

Publisher copyright

(Article begins on next page)

24 April 2024

Check for updates

Received: 1 June 2022 | Revised: 22 January 2023 | Accepted: 25 January 2023

DOI: 10.1002/esp.5555

RESEARCH ARTICLE

ESPL WILEY

Geophysical–geotechnical methodology for assessing the spatial distribution of glacio-lacustrine sediments: The case history of Lake Seracchi

Andrea Vergnano | Claudio Oggeri | Alberto Godio

Department of Environment, Land and Infrastructure Engineering, Politecnico di Torino, Turin, Italy

Correspondence
Andrea Vergnano, Department of Environment, Land and Infrastructure Engineering, Politecnico di Torino, Corso Duca degli Abruzzi 24, 10129 Turin, Italy.
Email: andrea.vergnano@polito.it

Funding information
"CC-Glacier lab" of the MIUR project "Department of excellence" at the Politecnico di Torino—DIATI

Abstract

Proglacial lakes are distinctive features of deglaciated landscapes and often act as sediment sinks, collecting solid material from subglacial erosion or washout of deglaciated areas. The solid transport flow, strongly linked to the glaciers and periglacial landforms, may rise due to the rapid changes driven by climate warming, causing deep transformations in the basin hydrology, and even the appearance or disappearance of lakes at a decadal timescale.

The goal of this study was to present a geophysical–geotechnical approach that integrates several techniques, to quantify the sediment distribution in a proglacial lake. A geophysical survey is performed with ground-penetrating radar (GPR) installed on a boat, whereas a time-domain reflectometer (TDR) measures the electrical conductivity and permittivity of the lakebed sediments. Unperturbed samples are collected and analyzed to measure the main geotechnical properties of the sediment: grain-size distribution, plastic limit, and liquid limit. Such properties support the interpretation of the GPR data and the detection of spatial variations of the sediment facies.

To validate the proposed methodology, field tests were carried out at Lake Seracchi, the largest lake of the Rutor glacier, Italian Alps. It formed around 1880 because of the recent glacier shrinkage, as chronicled by valuable historical documents. Its greyish waters carry a significant amount of suspended sediment recognized as glacial flour, which gradually accumulates on the bottom of the lake.

The obtained bathymetry and sediment thickness maps of Lake Seracchi show the strength of the approach: from only a few manual samples, it is possible to extrapolate the geotechnical properties of interest, such as friction angle or hydraulic conductivity, to wider areas, surveyed by the geophysical techniques. This is achieved by investigating the spatial distribution of key geophysical properties linked to the geotechnical properties of interest.

KEYWORDS
bathymetry, geotechnical–geophysical integrated methodology, glacio-lacustrine sediment properties, GPR, Lake Seracchi, Rutor glacier, sediment thickness, sedimentation

1 | INTRODUCTION

The proglacial environment refers to the areas located close to the ice front of a glacier, in which frost-driven geomorphic processes, called periglacial processes, may take place (Heckmann et al., 2019). Examples of multifaceted and interconnected aspects of proglacial geomorphology are deglaciated areas, permafrost, erosion, landslides, proglacial lakes, moraines, and vegetation colonization (Colombo et al., 2016; French & Harbor, 2013).

This is an open access article under the terms of the Creative Commons Attribution License, which permits use, distribution and reproduction in any medium, provided the original work is properly cited.
© 2023 The Authors. *Earth Surface Processes and Landforms* published by John Wiley & Sons Ltd.

10969837, 0, Downloaded from https://onlinelibrary.wiley.com/doi/10.1002/esp.5555 by CochraneItalia, Wiley Online Library on [14/02/2023]. See the Terms and Conditions (https://onlinelibrary.wiley.com/terms-and-conditions) on Wiley Online Library for rules of use; OA articles are governed by the applicable Creative Commons License

One of the most dynamic aspects of the proglacial environment is the formation and evolution of proglacial lakes. In the last century, many lakes gradually appeared in the deglaciated areas, barred by moraines, often in place of the previous glacier overdeepenings. As reviewed by Heckmann et al. (2016), proglacial lakes are an appealing scientific topic because they modify hydrological flow regimes, trap sediments, preserve a sedimentary archive of information about glacier behavior, sediment flux, and climate, and may be the theatre of devastating outbursts.

This paper focuses on the sediment storage role of alpine proglacial lakes—that is, the accumulation of a fraction of the suspended solids flowing in from the basin drainage network. This reduces and delays the sediment transfer from uplands to lowlands (Otto, 2019), and the recent formation of new proglacial lakes has had a great impact on downstream systems (Milner et al., 2017). Moreover, the proglacial lakes are subject to rapid modifications: if a large amount of sediment enters the lake over time, the lake may become filled with sediments (Bogen et al., 2015; Schiefer, 2006). A relevant case of formation and disappearance is that of the "Effimero Lake" (which means ephemeral, transient), which formed on the tongue of the Belvedere glacier, Macugnaga valley (northern Piedmont, Italy), after the fast changes in inflow rate due to the extraordinarily warm summer of 2002 (Tamburini & Mortara, 2005).

Among the geophysical surveys to investigate the bathymetry and sediment distribution of lakes, several techniques have been used, such as magnetic surveys, continuous vertical electric sounding (CVES), and ground-penetrating radar (GPR), other than conventional sonic and ultrasonic surveys (Sambuelli et al., 2011). Geophysical surveys are generally quicker to carry out compared to drilling and coring and may easily cover large areas, but lack ground-proof evidence of the investigated site. A combination of geophysical surveys and low-cost sampling is often an efficient way to gather enough information about the shallow subsurface.

GPR is particularly suitable for proglacial lakes, since it can penetrate several meters of depth if very low conductivity water derives from ice melting (Sambuelli & Bava, 2012). The thickness and coarseness of the sediments were detected by previous research on alpine lakes with GPR acquisitions (Lachhab et al., 2015; Sambuelli & Bava, 2012). GPR sections have been able to distinguish between different radar facies in similar contexts (Gomez & Miller, 2017; Pelpola & Hickin, 2004; Sambuelli et al., 2015; Shukla et al., 2008). GPR versatility has also allowed the detection of other interesting features of a lake—for example, vegetation, suspended solids (Qin et al., 2017) and thermal stratigraphy (Bradford et al., 2007). However, to the best of our knowledge, no study has ever combined geophysical and geotechnical measurements to test whether the different facies of lakebed sediment distinguished by point geotechnical measurements can be matched to some key geophysical properties of the sediment mapped over the entire lake area by geophysical surveys.

Therefore, the goal of the study was to test an integrated methodology, combining techniques from geophysics and geotechnics, to study the distribution of sediments over the entire area of a proglacial lake and recognize their different facies. It was intended as an expeditious (1–2 days), but thorough, alternative to a traditional coring survey. In our proposed methodology, the GPR travel times are constrained with time-domain reflectometer (TDR) measurements, since the electromagnetic wave velocity in the sediment is correlated to its average electrical permittivity, measured with a TDR at several locations throughout the lake. Geotechnical characterization of a few sediment samples is needed to constrain and confirm the geophysical data. Grain-size distribution, hydraulic conductivity, plastic limit, and liquid limit are obtained by following state-of-the-art methodologies as in the geotechnical literature (Casagrande, 1932; Taylor, 1948; Terzaghi et al., 1996). Such properties have been studied in previous literature to be related to the genesis of the glacio-lacustrine sediments and the processes they were subjected to (Boulton & Paul, 1976). The link between geophysical and geotechnical measurements is strong in the proposed methodology. The main hypothesis is that if a relation between geotechnical properties (e.g., grain-size distribution) and geophysical properties (e.g., electrical conductivity) was found, it would be possible to extend the information collected from the few sampling locations to a wider area covered by the geophysical survey.

This hypothesis was tested on the Lake Seracchi site (Valle d'Aosta region, Italian Alps), formed at the end of the 19th century due to the retreat of the Rutor glacier. Since that time, the subglacial erosion has produced a very fine glacier flour which, flowing in suspension, slowly sediments and accumulates at the bottom of the lake.

After sieving the sedimented glacier flour collected in a few locations, we found that its very fine grain-size distribution (silty clay) is the cause of an electrical conductivity higher than that of water. The high electrical conductivity, considered then as a proxy of the very fine grain-size distribution, was measured with the TDR probe to be high almost everywhere in the lake. Moreover, GPR reflections of the lakebed interface show a response that confirms the presence of fine sediment everywhere in the lake (more than 1.5 m thick, on average). Some exceptions were found, however. For example, in some limited areas near the inflows, the absence of fine sediment was observed in both samples and electrical conductivity, and was interpreted as the result of the higher water flow velocity, which does not allow the glacier flour to sediment. The data collected were combined to produce maps of the bathymetry and the sediment thickness of Lake Seracchi.

The combined geophysical–geotechnical methodology was tested to be fairly successful for addressing the purpose of mapping the geotechnical properties of proglacial lake sediments with a good balance between reliability, effort, and time.

2 | STUDY SITE

2.1 | Test site

The test site is the proglacial Lake Seracchi, situated in the Rutor glacier basin, Aosta Valley, Italy (Viani et al., 2020). A large amount of very fine suspended solids flows into it, coming from the subglacial erosion of the bedrock of the Rutor glacier and determining the peculiar greyish color of the lake. A percentage of the suspended solids has been trapped on the lake bottom since its formation, around 140 years ago. The Rutor basin is of historical importance, because of the past proglacial lake outbursts which greatly modified its hydrology and geomorphology (Sacco, 1917).

2.2 | Extended study site review

The Rutor massif is situated in the southwest of the Aosta Valley region, Italy (Figures 1 and B1). Its highest peak is called Testa del

10969837, 0, Downloaded from https://onlinelibrary.wiley.com/doi/10.1002/esp.5555 by CochraneItalia, Wiley Online Library on [14/02/2023]. See the Terms and Conditions (https://onlinelibrary.wiley.com/terms-and-conditions) on Wiley Online Library for rules of use; OA articles are governed by the applicable Creative Commons License

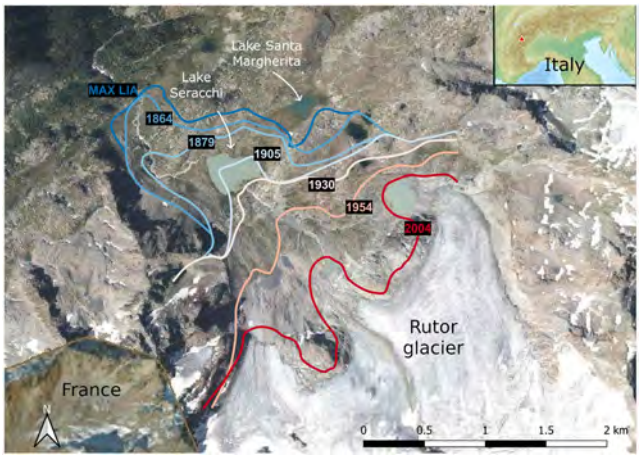

FIGURE 1 Map of the proglacial zone of the Rutor glacier. Colored lines indicate the glacier retreat after the Little Ice Age (LIA) according to the reconstruction by Villa et al, 2007). Orthophoto base map by Valle d'Aosta region, geoCartoSCT service (2018) (Regione Autonoma Valle d'Aosta, n.d.). Rendering by QGIS software

Rutor (*Tête du Rutor* in French); it is 3486 m a.s.l. and stands out over the homonymous glacier.

The most characteristic feature of the massif is the connection between the glacier and its several proglacial lakes (Monti, 1906). The Italian (northern) flank exhibits a series of five rock and moraine terraces, situated between 2000 and 2900 m a.s.l., in which lakes have successively formed and, in the upper part, are still forming due to the current glacier retreat (Preller, 1918). The progressive melting of the Rutor glacier since the Little Ice Age (LIA) maximum, reached around 1820 (Orombelli, 2005), deeply modified the basin landscape, leading to the creation or modification of existing proglacial lakes. This phenomenon has been recognized in several historical documents and scientific literature of different disciplines (Badino et al., 2018; Baretti, 1880; Carrel, 1867; Favre, 1867; Monti, 1906; Orombelli, 2005; Preller, 1918; Sacco, 1917; Viani et al., 2020). Most notably, the once biggest lake of the basin, Lake Santa Margherita, famous for sudden breakages of the ice dam that barred it, which have caused disastrous floods (glacial lake outburst floods, GLOFs) since 1500, starting from 1864 emptied itself (gradually, fortunately), from a 40 m deep lake to a 3 m deep lake (Preller, 1918). The changes in the glacier-covered area after the LIA were reconstructed from historical cartography by Sacco (1917), and more recently, by adding photogrammetry and GPR data, by Villa et al. (2007, 2008).

The formation of the proglacial Lake Seracchi dates to the period 1880–1920, as shown in cartographic maps and historical photos (Figures A1–A8; see Appendix A). Complete reviews of the Rutor basin with different scientific focuses, from geology to biology, were performed at the turn of the 19th and 20th centuries, and are an accurate and reliable reading to deepen knowledge about the area (Baretti, 1880; Carrel, 1867; Favre, 1867; Monti, 1906, 1929; Preller, 1918; Sacco, 1917). Notice that, in the literature, "Lago Rutor" or "Lac Ruitor" or similar names are used to refer both to Lake Seracchi and, perhaps more frequently, to Lake Santa Margherita.

Lake Seracchi has a rounded shape with a 300 m diameter, on average (area = 95,000 m^2), and it is situated at about 2385 m a.s.l. Unlike nearby lakes, like Lake Santa Margherita, which has clear water

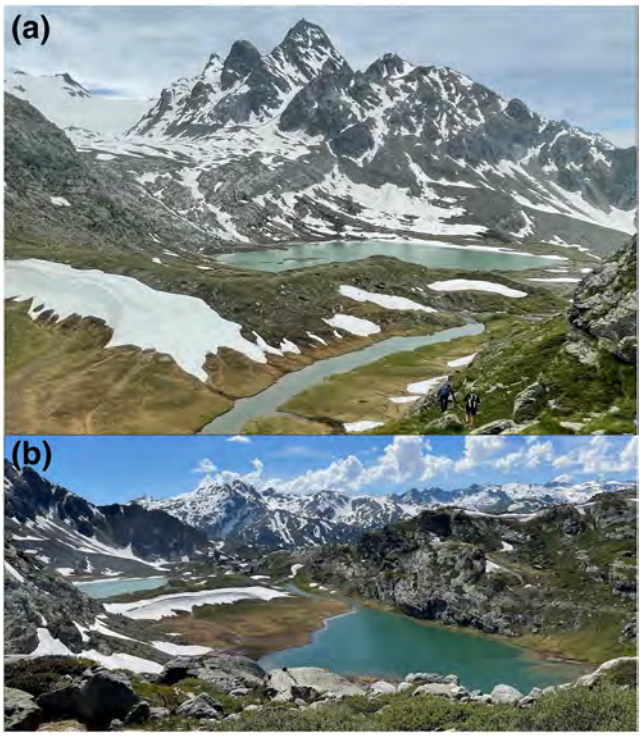

FIGURE 2 (a) Lake Seracchi (June 27, 2021). At the top left, a small portion of the Rutor glacier. At the bottom, the channel from Lake Santa Margherita to Lake Seracchi. Photo taken towards southwest at coordinates WGS 84 UTM 32 N 342953 5059737. (b) Lake Seracchi (top left) and Lake Santa Margherita (right). Note the color difference of the waters under the same sky. Photo taken towards northwest on June 26, 2021, at coordinates WGS84 UTM 32 N 343477 5059647. Photos courtesy of Elisabetta Corte

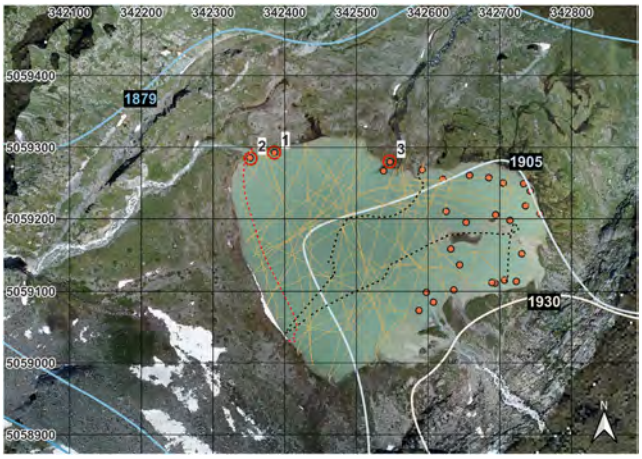

FIGURE 3 Map of the GPR, TDR and sampling survey. In yellow, the route of the boat carrying the GPR antenna. In red, the GPR line (#29) shown in Figure 6b (path direction from south to north). Some traces were removed due to GPS inaccuracies (black dashed lines). In orange, the locations of TDR probe point measurements. Red circles indicate the three manual sediment samplings, carried out in October 2021. GPS accuracy: ±3 m. Orthophoto by drone photogrammetric survey (resolution 6 cm), taken in July 2021. The years and lines refer to the glacier shrinkage that caused the formation of the lake. Rendering by QGIS software. CRS: WGS84 UTM 32 N

10969837, 0, Downloaded from https://onlinelibrary.wiley.com/doi/10.1002/esp.5555 by CochraneItalia, Wiley Online Library on [14/02/2023]. See the Terms and Conditions (https://onlinelibrary.wiley.com/terms-and-conditions) on Wiley Online Library for rules of use; OA articles are governed by the applicable Creative Commons License

and a green color, Lake Seracchi has always (Monti, 1906) had a peculiar tint (see Figures 1, 2a, 2b, and 3) due to its turbidity. A large amount of very fine suspended solids comes from subglacial erosion from the Rutor glacier, which provides for the lake waters. Part of it remains suspended in the lake waters until the outflow, reducing the water transparency. A part settles on the bottom of the lake, gradually filling it. This peculiar greyish color, due to the suspended solids of glacier provenance, is also reviewed by Karlén in Lapland and this material can be called "glacial flour", "glacier flour" or "rock flour" (rock flour|National Snow and Ice Data Center, n.d.; Karlén, 1981). The sedimentation process of Lake Seracchi is of particular interest, because it may change its morphology and hydrodynamics, eventually causing the complete disappearance of the lake. Since it is currently the major water reserve in the basin, eventual changes will affect the hydrological cycle of the whole valley.

The study site is rich in geomorphological features and has sparked the interest of researchers since the second half of the 19th century. Interesting studies also exist in the recent literature. The geometry changes of the retreating Rutor glacier were used to calibrate a plugin for QGIS software to model glacier behavior under climate change (Strigaro et al., 2016). Viani et al. (2020) studied this area to calibrate a procedure, based on the GlabTop2 model (Linsbauer et al., 2012), to forecast the formation of future lakes in the place of current glacier overdeepenings. The shrinking of the Rutor glacier locally revealed peat outcrops (Armando & Charrier, 1985), helpful for depicting the evolution of climate and vegetation of the Rutor basin in the past 8800 years (Badino et al., 2018). Local springs are reporting an increase in water discharge in the last years (Gizzi et al., 2022).

3 | METHODS

3.1 | Ground-penetrating radar

GPR technology is based on emitting electromagnetic waves towards the ground subsurface or other materials, and measuring the travel time needed for the signal to be reflected back to the instrument. These reflections occur when the signal traveling in a material encounters the interface of another material with different electrical permittivity. By moving the instrument on the ground and plotting multiple signals next to each other, one can display subsurface *x*-depth sections, where interfaces such as the water table or the bedrock are plotted as continuous lines. The GPR is able to survey the lake bathymetry and investigate the thickness of the deeper sediment layer, as reported in previous studies (Lachhab et al., 2015; Mihu-Pintilie et al., 2016; Sambuelli et al., 2011, 2015; Sambuelli & Bava, 2012; Sambuelli et al., 2009). However, one must pay attention to many factors such as the high density of underwater macrophytes or the high concentration of suspended sediments, which can introduce noise challenging the quality of the radargrams (Tretjakova et al., 2019). Besides, visual observation of reflection patterns, or even advanced geostatistical techniques, may detect the correlation structure of the subsurface, in order to distinguish different facies and orientations of the layers (Rea, 1996).

A GPR antenna was mounted on an inflatable rowing boat. The GPR antenna model was a TR 200 KR, manufactured by IDS, having a shielded dipole with a central frequency of 200 MHz; it was 42 cm long and 37 cm wide. It was connected to a control unit to record and digitalize the acquired data; the raw radargrams were saved on a PC unit, as shown in Figure B2 in Appendix B.

The time window for each trace was initially set to 600 ns (a two-way travel time corresponding to about 10 m in water) but was raised to 1200 ns from GPR line #5 onwards, since the lake was found to be deeper than the maximum depth reached with 600 ns.

The profiles covered the whole lake area, as shown in Figure 3, and the survey required 2 days to complete. A pair of GPR lines (42nd and 43rd) were not considered in this phase due to inaccuracies in the GPS positioning.

Basic postprocessing was required to optimally visualize the GPR sections; it was carried out with ReflexW commercial software (Sandmeier, 2012). The main steps of the data processing are summarized as follows:

- The start time of each trace was moved, deleting the signals before the main bang, to obtain an accurate zero time.
- The subtract-mean filter, also called the dewow filter, which sets the average amplitude value of each trace equal to 0, was applied to remove the low-frequency part of the signal.
- The background removal filter, which subtracts the average trace from each trace, was applied to remove some coherent instrumental noise.
- The gain was increased as a function of depth, to soften the effects of the signal geometrical spreading (divergence compensation).
- The electromagnetic wave velocity in water was considered equal to 0.03287 m/ns, for a time-to-depth conversion. This value was calculated from the measured average value of the electrical permittivity (83.3) using Equation (1). The value seems reasonable according to the temperature dependence of the electric permittivity of water and the observed temperature of 6°C (Hill, 1970).
- The reflective interfaces visible in the GPR sections were manually picked. Two interfaces were visible, the first representing the lake bottom and the second interpreted as the bottom of the sediment layer.
- The radar reflection relative to the water–sediment interface was difficult to detect where the water depth was highest. Other processing techniques were useful to display the interface clearly, such as lowpass filter (cutting frequencies higher than 200 MHz, more subject to dispersion in water; Bradford et al., 2007), stacking of adjacent traces, background removal filter over small sections.

Bathymetric and sediment-thickness maps were obtained by interpolating the GPR pickings of the reflection events. The interpolation procedure was based on a triangulation-based linear interpolation method, considering the lake boundary as values equal to zero water thickness. The lake borders (perimeter) were drawn in a QGIS environment, from a 6 cm resolution orthophoto by drone photogrammetric survey taken in July 2021 (see Figure 3).

A brief survey (two GPR lines) of the near Lake Santa Margherita, a tributary of Lake Seracchi, was performed to estimate the average depth of this shallower lake and to compare its radar facies with those observed in Lake Seracchi.

10969837, 0, Downloaded from https://onlinelibrary.wiley.com/doi/10.1002/esp.5555 by CochraneItalia, Wiley Online Library on [14/02/2023]. See the Terms and Conditions (https://onlinelibrary.wiley.com/terms-and-conditions) on Wiley Online Library for rules of use; OA articles are governed by the applicable Creative Commons License

3.2 | Time-domain reflectometer

A TDR probe is a two-rod, 15 cm long probe capable of measuring both the electrical conductivity and the dielectric permittivity of liquids and porous materials (Vergnano et al., 2019). The average dielectric permittivity of the fine sediments was measured via Equation (1) to estimate the propagation velocity v of GPR signals:

$$v = \frac{c}{\sqrt{\varepsilon_r}}, \tag{1}$$

where c is the electromagnetic wave velocity in a vacuum and ε_r is the relative dielectric permittivity of the sediments (Psarras, 2018).

The measurements were performed all around the lake, where the water depth was shallow enough to firmly insert the probe in the sediment, with the help of a 2-m rod. A few measurements near the inflows (from Lake Santa Margherita on the north side, and from Rutor glacier on the south side) were performed to investigate eventual differences in the quality of the sediments compared to the sediment deposited throughout the lake.

3.3 | Geotechnical characterization

The geotechnical characterization of the glacier flour of Lake Seracchi confirms the indirect geophysical measurements, especially regarding the grain-size distribution and the presence of clay-sized particles, the latter being responsible for high electrical conductivity, which in this methodology is measured with the TDR. Moreover, the geotechnical properties are relevant in discussing the sedimentation and rearrangement processes that occurred in the past and the expected behavior in terms of stiffness and hydraulic conductivity. Suggestions from soil mechanics indicate that at least grain-size distribution and plasticity features should be investigated for samples collected in different representative zones of the area and, possibly, at different depths (Ameratunga et al., 2016). These experiences are auxiliary also for the determination of strength properties with regard to any further process involving water streams, loading, unloading, etc. Another main purpose of integrating the geotechnical characterization in our methodology is the possibility to extrapolate the geotechnical properties, measured in a few locations, to the larger areas surveyed by the geophysical instruments.

The sampling of lakebed sediments was performed in October 2021 in three locations highlighted in the map in Figure 3, which are, from west to east:

- near the emissary, where the outflow water velocity was maximal (sample 2 in Figure 3);
- 40 m away from the emissary, in an area of calm water (sample 1 in Figure 3);
- at the inflow from the tributary channel coming from Lake Santa Margherita (sample 3 in Figure 3).

For the first two, a manual core drill was used to collect undisturbed samples of the fine sediments. The latter, much coarser, was simply collected without maintaining its volume.

The following main features can be summarized.

The porosity (n) of the collected samples was calculated in a laboratory, considering them as 100% saturated by water, by weighing them in wet conditions and after oven drying for 24 h.

Particle size distribution was carried out by sieving. Sieve dimensions for the fine sediments (mm) were 0.04, 0.025, 0.01, and 0.002.

The geotechnical properties analyzed in the following—the Atterberg's limits (liquid and plastic limit, LL and PL)—deal with the mechanical behavior of the material and its consolidation state. The liquid limit and plastic limit represent the water content associated with the macroscopic change of behavior as the "physical state" of granular material, respectively from plastic to liquid and from semisolid to plastic. The Atterberg's limits are parameters very helpful in case the methodology is applied to sites at risk of a GLOF or other failures, where sediments can mobilize into sediment floods. The liquid limit of the material—that is, the water content at which the material passes from the plastic state to the liquid state—was determined by adopting Casagrande's method, according to the procedure of ASTM standard test method D 4318 (D18 Committee, 2018). To calculate the plastic limit of the material—that is, the water content at which the material passes from the semisolid state to the plastic state, the moisture content at which a 3.2 mm diameter thread of sediment sample broke apart was measured, according to the procedure of ASTM standard test method D 4318 (D18 Committee, 2018). The plasticity index (PI) is the difference between LL and PL. The greater the PI, the greater the apparent stability of the granular material during water content changes (desiccation, saturation, flooding, drainage, etc.).

The hydraulic conductivity under saturated condition (k) can be related to the porosity, according to the studies by Clarke (2018) and Al-Moadhen et al. (2020), which refer to an equation form proposed by Chapuis and Aubertin (2003), for very fine glacio-lacustrine deposits:

$$k = 1 \times 10^{-10}\left[\frac{1}{LL^2}\cdot\frac{e^3}{1+e}\right]^{1.58}, \tag{2}$$

where LL is the liquid limit, and e is the void ratio $= n/(1-n)$.

The eventual presence of carbonates was tested by acid attack: a small quantity of hydrochloric acid (0.1 N) was dropped onto a small portion of the fine sediment to see if it fizzed.

4 | RESULTS

4.1 | Ground penetrating radar and time-domain reflectometer

In Figure 4, the main results are presented. The GPR-TDR combined survey allowed us to draw a bathymetry map (Figure 4a) and a sediment thickness map (Figure 4b). The supporting TDR measurements of electrical permittivity and conductivity are shown in Figures 4c and 4d, respectively.

The bathymetry map in Figure 4a shows that, all over the eastern part, the lake is 1–3 m deep. In the western part two large overdeepenings are found of about 80–120 m, with a maximum depth of almost 11 m. The result is representative of the July 2021 situation.

10969837, 0, Downloaded from https://onlinelibrary.wiley.com/doi/10.1002/esp.5555 by CochraneItalia, Wiley Online Library on [14/02/2023]. See the Terms and Conditions (https://onlinelibrary.wiley.com/terms-and-conditions) on Wiley Online Library for rules of use; OA articles are governed by the applicable Creative Commons License

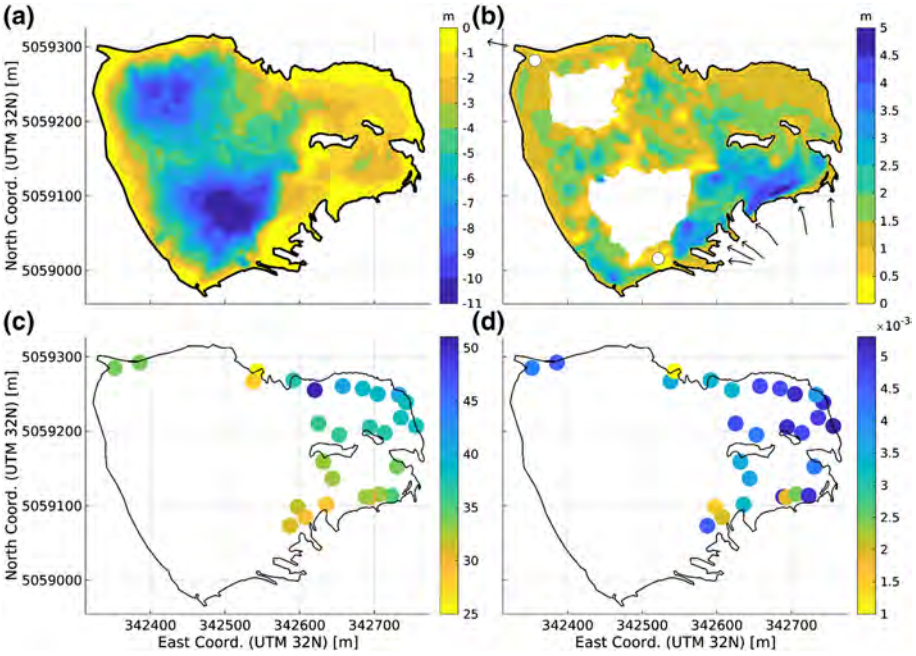

FIGURE 4 (a) Interpolated contour map of the lake bathymetry by GPR survey. (b) Interpolated thickness distribution of fine sediments at the bottom of Lake Seracchi. White circles indicate the coarse debris surfacing indicated in Figures 6b and 7. In two large areas of the lake (approx. depth > 7 m) the signal was highly attenuated by the thick water layer: No reliable data were recorded there. The arrows indicate the main inflows (south: from the glacier; north: from lake Santa Margherita) and the outflow of the lake. (c) Relative dielectric permittivity of sediments from TDR measurements. (d) Electrical conductivity (S/m) of sediments from TDR measurements. The georeferenced maps and data in this figure are available in the Supporting Information

FIGURE 5 Photography of the border of the lake in October 2021, showing its seasonal changes. The water surface is covered by a thin frozen layer that will grow thicker in the winter (photo taken from coordinates WGS84 UTM 32 N 342392 5059300)

The total volume of water in the lake was about 370,000 m^3 in July 2021, with an average depth of 3.9 m and a maximum depth of almost 11 m, consistent with previous literature (Monti, 1906). During the second survey in October 2021, for example, the water level was about 20 cm below that of July 2021, and the lake perimeter shrunk by several meters, uncovering part of the lakebed. See Figure 5, taken in October; in July the water bordered the grass.

The fine sediment was found almost everywhere in the lake, mostly with a thickness of at least 1 m, as shown in Figure 4b. Notable is the major accumulation of fine sediments in the southeastern part of the lake, where the main inflows from the Rutor glacier are located. To calculate the thickness of the sediment layer from the two-way travel time of the GPR signal, an estimation of the electromagnetic wave velocity was needed. The average value of the electrical permittivity representative of the fine sediment was measured with the TDR probe to be about 36 ± 3 (Figure 4c), which brings, according to Equation (1), a velocity of the electromagnetic waves in the sediment of about 0.05 m/ns (maximum estimated error = 15 cm where the thickness = 4 m). Lower values of 25–30, not included in this average, were detected in a radius of a few meters near the inflows, where the sediment was coarser. One measurement, over 50, is probably affected by the only partial driving of the probe in the sediments: the observed value is also dependent on the higher (over 83) dielectric permittivity of water, and it was considered an outlier. Not all GPR sections reliably showed the second interface, especially for water depth greater than 6–7 m, where the water column provided intense signal attenuation. Therefore, in Figure 4b, the two large areas of uncertain sediment thickness are not depicted in any color. The total volume of sediments is about 150,000 m^3, obtained by multiplying the average thickness of about 1.6 m (average made excluding the uncertain areas) by the area of the lake. The electrical conductivity measurements reproduced a similar trend for permittivity (Figure 4d). However, the difference between the fine sediment (higher conductivity) and the coarser sediments (lower conductivity) near the inflows was more pronounced compared to that of the electrical permittivity. The high value of conductivity is supposed to be due to the presence of a high percentage of clay-sized particles in the fine sediment, as proven by the grain-size distribution analysis discussed in the following paragraphs. Electrical conductivity is therefore found to be a more suitable parameter to distinguish the kinds of sediment in this test site compared to the permittivity. Near the inflow from Lake Santa Margherita, the electrical conductivity was measured at two points: where the coarse sediment was taken, and a few meters away into the lake. The latter measurement reported an electrical conductivity intermediate between the coarse sediment and the fine ones, and some mixing of the different kinds of sediments was visually observed. At those two points, the dielectric permittivity showed similar behavior to that of conductivity: from TDR measurements, and backed by theory (Milton, 2018), also the dielectric permittivity is higher in clayey sediments than in coarse ones, although with a smaller difference compared to the electrical conductivity.

10969837, 0, Downloaded from https://onlinelibrary.wiley.com/doi/10.1002/esp.5555 by CochraneItalia, Wiley Online Library on [14/02/2023]. See the Terms and Conditions (https://onlinelibrary.wiley.com/terms-and-conditions) on Wiley Online Library for rules of use; OA articles are governed by the applicable Creative Commons License

The electrical permittivity of the water was measured as 83.8, the electrical conductivity was 0.0016 S/m, and the water temperature at the surface was 6°C (July 10, 2021, at around 3 p.m., on a sunny day).

The TDR measurements and their locations are also available in Table B1 in Appendix B.

4.2 | GPR detection of different sediment facies

To produce the maps in Figures 4a and 4b, the GPR sections were analyzed to detect the water–sediment interface and a second interface below the first. An example is shown in Figure 6a, where the two different reflections are clearly visible. A pronounced thinning of the fine sediment layer can be observed in a few GPR sections, showing a surfacing of probable coarser sediments. An example is given in Figure 6b. A photography survey (Figure 7) confirmed the presence of gravel and stones 10–100 cm thick in those locations, highlighted with circles in Figure 4b, confirming the capability of the 200 MHz GPR to distinguish (very) different kinds of material in this environment.

4.3 | Comparison of GPR sections with Lake Santa Margherita

To test the applicability of the GPR system used in Lake Seracchi to other lakes, a brief comparison is here introduced with the nearby Lake Santa Margherita (Figure 8).

Lake Santa Margherita, identifiable in Figures 1 and 2b, is a tributary of Lake Seracchi, and it has characteristics and history very different from Lake Seracchi, even if they are only 500 m away. Lake Santa Margherita has more transparent and greenish waters, indicating vegetation activity, which contributes to the accumulation of organic sediments on the lakebed. This lake is indeed not the source of the fine sediments of Lake Seracchi, which come instead from the southern inflows—that is, from the Rutor glacier. Detailed information on this lake is found in historical literature (Monti, 1906; Preller, 1918; Sacco, 1917).

In GPR sections of Lake Santa Margherita, the fine sediment/coarse sediment interface is not pictured, even if the very shallow water (average: about 1 m deep) should not greatly attenuate the radar signal. Therefore, while the lake bottom is clearly displayed, no reliable information can be extracted about the sediment layer, showing only some sparse reflections. The observed response to the radar signal is quite different from the GPR sections of Lake Seracchi (Figures 6a and 6b), where the sediment layer is clearly detected. This is supposed to be due to the different nature or structure of the sediment layers. One hypothesis is that, whereas now Lake Santa Margherita does not collect any glacial flour or turbid waters, it did probably in the colder past, when it was the only lake in that terrace of the basin and it collected water coming directly from the Rutor glacier. This lake, thus being much older than Lake Seracchi, could have accumulated a thicker layer of sediments—too thick to be investigated

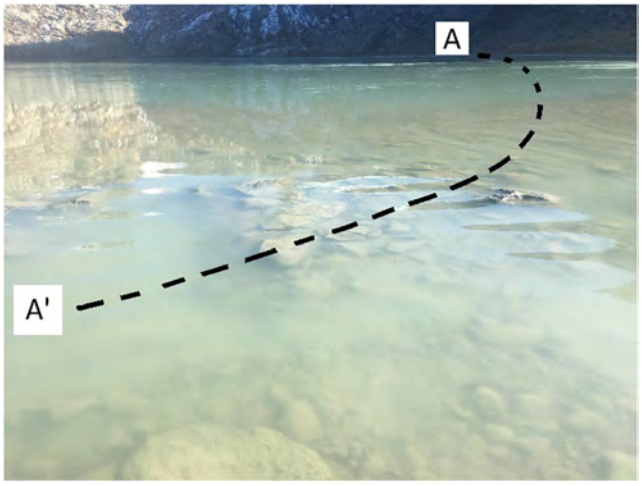

FIGURE 7 Lakebed near the lake emissary on October 25, 2021 (coordinates: WGS84 UTM 32 N 342353 5059292). Since the water level of the lake was about 20 cm lower than in July 2021, the coarse debris appeared clearly below the shallow turbid water. The diameter of this coarse debris is 10–100 cm, and was detected by the GPR survey in Figure 6b—see the dashed line A–A′ and also the GPR section #29 in Figure 3. In most other parts of the lake side, only fine sediments are visible, except from the inflows where gravel and pebbles are present and another large debris area indicated by a white circle in Figure 4b

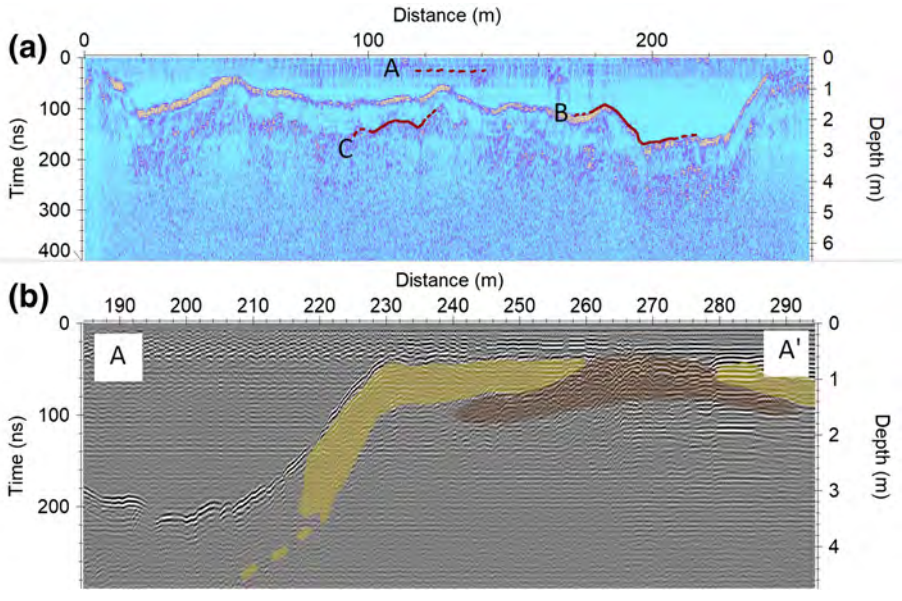

FIGURE 6 (a) Example of a GPR section in which the different reflections are particularly clear. A: Noise due to paddling and boat movement. B: Lake bottom–fine sediment interface. C: Fine sediments–coarse debris interface. (b) Zoom of GPR section #29. Note the thinning of the fine sediment layer (in yellow) at distance = 260–280 m. As the boat approached the lake outflow, subsidized coarse debris (in brown) began to appear (see also the photo in Figure 7, the GPS route #29 in Figure 3 and the location of the coarse sediment surfacing in Figure 4b)

10969837, 0, Downloaded from https://onlinelibrary.wiley.com/doi/10.1002/esp.5555 by CochraneItalia, Wiley Online Library on [14/02/2023]. See the Terms and Conditions (https://onlinelibrary.wiley.com/terms-and-conditions) on Wiley Online Library for rules of use; OA articles are governed by the applicable Creative Commons License

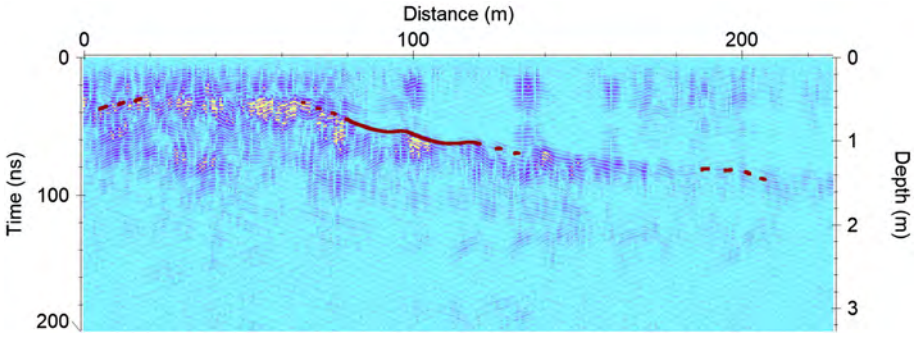

FIGURE 8 Example GPR section from the center of Lake Santa Margherita, surveyed in July 2021

TABLE 1 General information about the fine sediment sampling carried out in October 2021

Sample location	UTM E (WGS84 UTM 32 N)	UTM N (WGS84 UTM 32 N)	Core barrel length/ diameter (cm)	Dry weight (DW) (g)	Saturated weight (SW) (g)	DW/ SW	Total volume (cm^3)	Porosity *n* (%)
Calm water	342385	5059293	13/5	350	476	0.73	255.3	49
Emissary	342352	5059284	7/5	165	236	0.7	137.4	52

with the relatively high-frequency antenna employed in this study. Another hypothesis is that the fine sediments were mobilized during the past outbursts and the GPR, today, observes a layer of different nature. This could be confirmed by sampling the Lake Santa Margherita sediments.

4.4 | Sampling of fine sediment and geotechnical analyses

The sediment samples manually collected are representative of the finer part of the glacier-eroded sediment. It is free to move in suspension according to the water flow and has accumulated all over the lake, except for the small areas near the inflows where the velocity is too high to let it deposit. These fine sediment samples have been analyzed to obtain the grain-size distribution and the main geotechnical properties, in order to support the interpretation of the GPR and TDR surveys. A summary of the general information on the fine sediments is presented in Table 1.

The differences in the comparable parameters, such as dry weight/saturated weight or porosity, are estimated to be inside the range of measurement error: the two samples are quite similar. The same consideration can be made for the grain-size distribution, shown in Figure 9.

The prevalence of fine classes in the grain-size distribution of the collected sediments allows us to classify them as silty clays. The scattering of values between the two samples is quite low, even if one sample was collected where the water was calm and the other at the emissary, where the water flow was fairly fast. For this reason, and for the uniformity of TDR measurements, this local sampling can be considered representative of the fine sediment accumulated all over the lake bottom. According to the classification of glacial comminution processes proposed by previous literature, the glacial flour of Lake Seracchi comes from abrasion processes of the glacier bedrock (Dreimanis & Schlüchter, 1985; Haldorsen, 2008), consisting of metamorphic rocks such as arenaceous and conglomeratic schists, or mica and garnet schists (Badino, 2016). According to Haldorsen (1978), the

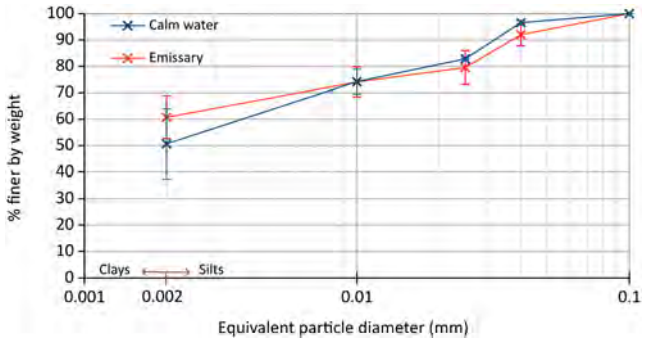

FIGURE 9 Grain-size distribution of the samples collected at the beginning of the emissary and in a calm water area. In the graph, it was hypothesized no grain was greater than 0.1 mm. Sieve dimensions (mm): 0.04; 0.025; 0.01; 0.002

glacial comminution processes may produce very fine particles if the bedrock contains crystalline minerals, whereas sedimentary bedrock is more resistant to fine comminution and, in general, it is simply reduced to the grain-size composition of the parent rock. The former seems to be the case for the glacial flour observed in Lake Seracchi, which is mainly composed of mica and quartz according to a preliminary optical microscope screening.

The calm-water sample was measured to have the plastic limit at water content $W = 23.2 \pm 2.8\%$, and the emissary sample at $W = 22.0 \pm 1.9\%$. The average was done on four samples. The results of the liquid limit analysis are reported in Figures 10a and 10b.

In Figure 11a the classification of the two samples is shown in Casagrande's chart, based on their plasticity index and liquid limit. Available literature correlations show that clay tills and glacial deposits fall within this range, as shown in Figure 11b (Sorensen & Okkels, 2013).

According to the Unified Soil Classification System, the sediment types of Lake Seracchi are ML-CL (*Standard Practice for Classification of Soils for Engineering Purposes* (*Unified Soil Classification System*), n.d.) (M stands for silt, C for clay, and L for low liquid limit).

Neither fine-sediment sample, when attacked by hydrochloric acid, reacted visibly, showing low content of carbonates.

10969837, 0, Downloaded from https://onlinelibrary.wiley.com/doi/10.1002/esp.5555 by CochraneItalia, Wiley Online Library on [14/02/2023]. See the Terms and Conditions (https://onlinelibrary.wiley.com/terms-and-conditions) on Wiley Online Library for rules of use; OA articles are governed by the applicable Creative Commons License

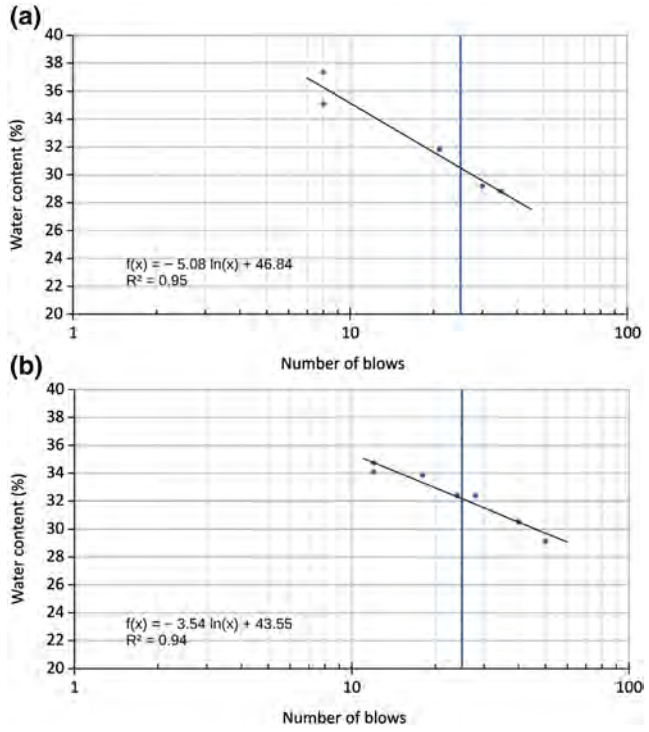

FIGURE 10 (a) Results of Casagrande's method for calculating the liquid limit of the calm water sample. The liquid limit water content corresponds to that at 25 blows (blue vertical line) = 32.2. (b) Results of Casagrande's method for calculating the liquid limit of the emissary sample. The liquid limit water content corresponds to that at 25 blows (blue vertical line) = 30.5.

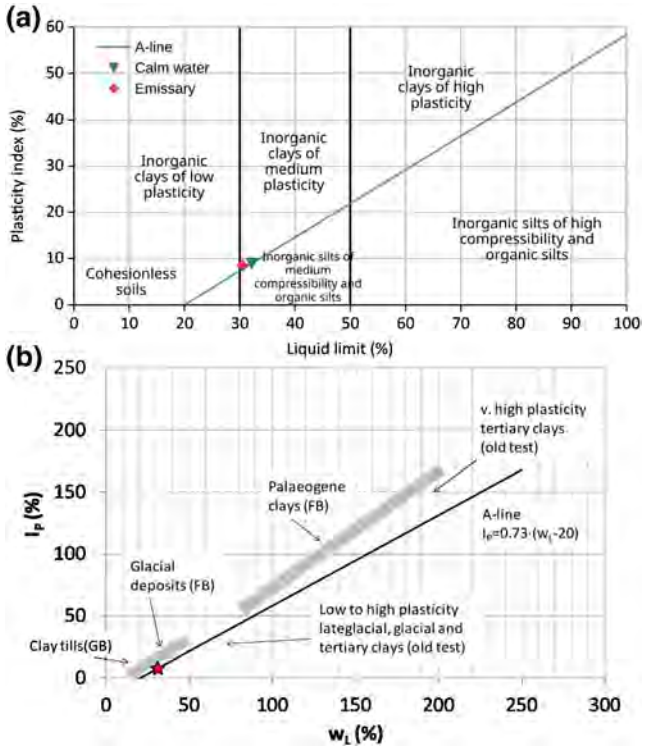

FIGURE 11 (a) Casagrande's chart (Casagrande, 1932; Terzaghi et al., 1996). The two samples are in the area of inorganic clays of medium plasticity, very near to the area of inorganic silts. Indeed, from the grain-size distribution analysis, the samples are about 50% silty and 50% clayey. (b) Casagrande's classification chart IP versus W_L (modified after Sorensen & Okkels, 2013). Red asterisk represents the Lake Seracchi sediment, which falls in the range of previous literature, confirming proper classification and lab procedure.

4.5 | Coarser sediment sampling

The sediments near the inflows can be different compared to those present all over the lake, and Lake Seracchi is no exception, as detected with the TDR measurements. To confirm and characterize this kind of coarser sediment, another sample was collected at the tributary inflow from Lake Santa Margherita (WGS 84 UTM 32 N 342546 E, 5059280 N) with total weight = 1779.4 g. Sieving analysis was performed to obtain the grain-size distribution curve shown in Figure 12.

The grain-size distribution curve in Figure 12 is found to be well graded, without any step; the uniformity coefficient D_{60}/D_{10} is very high: about 16. According to the Unified Soil Classification System, it is of class GW, which is well-graded gravel, a poorly sorted sediment. This evidences a geologically short (150 years) timescale transport, in which the little fluvial reworking has not strongly classified the material. Owing to the large diameter of grains, this sediment cannot move for more than a few meters into the lake, and remains confined in the areas of the inflows. This is coherent with the TDR measurements at the inflow from Lake Santa Margherita, which evidenced a lower electrical conductivity only in the radius of a few meters around the inflow.

4.6 | Open access and reproducibility statement

All the results have been made available as an open dataset on the Zenodo repository for future reuse (Vergnano, Godio, & Oggeri, 2022b).

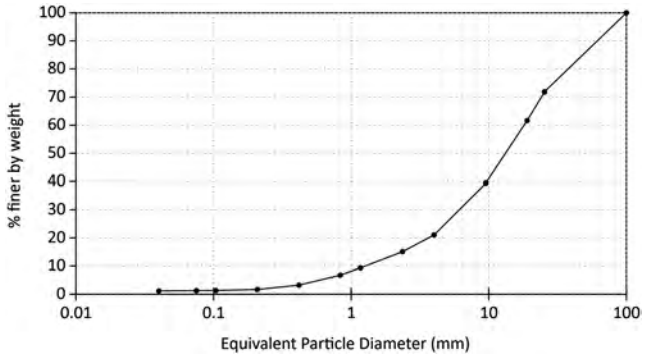

FIGURE 12 Grain-size distribution of the sample collected at the tributary from Lake Santa Margherita. In the graph, it was hypothesized that no grain was greater than 100 mm. Total weight of the sample was 1779.4 g.

5 | DISCUSSION

5.1 | Bathymetry

The GPR survey on Lake Seracchi easily pictured the water–sediment interface after post-processing of the radar data. In the GPR sections, reflections coming from the possible thermocline, as observed in previous research (Bradford et al., 2007), were not displayed. This is

10969837, 0, Downloaded from https://onlinelibrary.wiley.com/doi/10.1002/esp.5555 by CochraneItalia, Wiley Online Library on [14/02/2023]. See the Terms and Conditions (https://onlinelibrary.wiley.com/terms-and-conditions) on Wiley Online Library for rules of use; OA articles are governed by the applicable Creative Commons License

confirmed by the measurement of lake temperature, which is already low at the surface (about 6°C on July 10, 2021, at around 3 p.m., with direct sunlight). This observation is in agreement with a previous study, which evidenced that turbid lakes have lower temperatures, on average (Koenings & Edmundson, 1991). Other radar reflections due to vegetation, such as those described by Mihu-Pintilie et al. (2016), were also not displayed. This is consistent with the nature of the lake: its suspended solids concentration does not allow vegetation to thrive, as the absence of organic matter in the manually collected samples confirms. The presence of suspended sediments itself had challenged in past surveys the resolution of the GPR sections (Tretjakova et al., 2019); however, in this study, this problem has not been encountered.

This method, with a 200 MHz antenna, on low-conductivity water, is expected to reach a maximum investigation depth of 15 m. Note that accuracy limitations may come not only from too deep water but also from too shallow water. In fact, the marginal areas, where the water was up to 20–30 cm deep, were arduous to investigate with our boat setup. In these areas, the reported bathymetry comes from interpolation more than from data, but this error does not significantly affect the total volume estimation. If more accuracy is needed for shallow-water areas, other survey procedures must be employed. The survey could be carried out by walking with fisherman's boots, but in our case, the sticky nature of the sediment made walking impossible and dangerous. A small unmanned boat can be employed in those cases, or an airborne survey could be tested, carrying the GPR antenna on a drone at 1–2 m above the water, as performed for other applications (Vergnano, Franco, & Godio, 2022a).

5.2 | Sediment thickness and spatial distribution of sediment facies

The thickness of the sediments was, as expected, more difficult to retrieve from the GPR sections compared to bathymetry, especially where the water was deeper than 6–7 m, due to signal attenuation. The full applicability of the methodology proposed, therefore, is expected to be possible only for proglacial lakes less deep than 5 m. However, the GPR is not only able to retrieve the sediment thickness but also the sediment radar facies, namely the qualitative shape and distribution of the radar reflections, which allowed us to distinguish fine from coarse lakebed in Figure 6b. Overall, in our test site, fine sediment facies were distinguished almost everywhere in the lake. The sediment radar facies distribution could be retrieved for depths up to 10 m with the employed setup, by analyzing only the first meter of the sediment layer and not its full thickness, enhancing the applicability of the methodology (although with limited results).

The TDR measurements of electrical permittivity supporting the GPR survey proved successful in estimating the electromagnetic wave velocity in the sediments and therefore their thickness. Some authors have adopted the diffraction hyperbolae technique to retrieve the sediment velocity in lacustrine environments (Sambuelli & Bava, 2012), but in the GPR sections of Lake Seracchi they were hardly visible. Probably, the fine sediment layer is quite homogeneous, and large objects such as rocks are absent in most parts of the lake. In this and similar cases, combining the GPR survey with some TDR point measurements is a more reliable and consistent way to estimate the electromagnetic wave velocity.

The TDR measurements of electrical conductivity, jointly with the grain-size distribution of the samples, were useful to understand the nature of the fine sediments and confirm their facies distribution from the GPR survey. In Lake Seracchi, the sediments are very fine, being composed mainly of silt and clay-size particles (Figure 9). According to the TDR measurements, in most parts of the lake the sediment electrical conductivity is about 0.003–0.004 S/m—higher than that of water (0.0016 S/m). This higher conductivity is probably due to the presence of ions on the surface of clay-size grains (Qi & Wu, 2022; Ward, 1990). In two small areas (a few square meters) in the very proximity of the inflows, the electrical conductivity of the sediment is lower than the average 0.003–0.004 S/m (Figure 4d). There, the electrical conductivity is comparable to that of water (0.0016 S/m). This is due to the different nature of the sediments: in these zones, the sediment is coarser (sand–gravel), because the water velocity is sufficient to transport heavier grains and it does not allow the fine part to sediment.

The electrical conductivity measurements of the TDR and the thickness distribution obtained with the GPR may be interpreted together to bring interesting results. The map in Figure 4b shows that in the southeast part of the lake; that is, at the inflows from the glacier the accumulated sediments form a thicker layer. In the same area, spots of lower electrical conductivity detect the presence of coarser sediments near the inflows. Therefore, it is expected that the whole southeast area has been subjected to the accumulation of both fine and coarser sediments, distributed according to the distance from the inflow. This behavior is commonly observed in lakes: only near the inflows, where typically the kinetic energy is higher, can the coarser particles be transported, creating a spatial differentiation of the grain-size distribution (Inman, 1949). Moreover, in different periods of the lake history, there have probably been changes in the inflow positions due to the sedimentation process itself and due to modification in the Rutor glacier extension. From the GPR sections, this difference in the facies of sediments in the southeast zone is not visible, probably due to the low resolution of the antenna (which, in water, has a wavelength of about 165 mm—much greater than the expected size of the coarser sediments). However, the coarser gravel sediments are expected to be present only in the proximity of inflows, thanks to the TDR measurements. Instead, GPR managed to distinguish where the debris has a much greater diameter, from 10 to 100 cm, in the two zones evidenced in Figures 4b, 6b, and 7.

Similar considerations can be made about the dielectric permittivity distribution in the lake, even if, in this test site, the electrical conductivity was more suitable to distinguish the clayey sediments, due to its higher sensitivity to clay presence compared to the permittivity.

5.3 | The role of geotechnical properties in integrated methodology

In the proposed methodology, the interpretation of the GPR-TDR survey is supported by ground-proof data. For example, TDR measurements showed that the sediment has an electrical conductivity higher than that of water—a behavior often found in the presence of clay.

10969837, 0, Downloaded from https://onlinelibrary.wiley.com/doi/10.1002/esp.5555 by CochraneItalia, Wiley Online Library on [14/02/2023]. See the Terms and Conditions (https://onlinelibrary.wiley.com/terms-and-conditions) on Wiley Online Library for rules of use; OA articles are governed by the applicable Creative Commons License

The grain-size distribution analysis performed is able to confirm this hypothesis.

At the same time, the GPR and TDR combination was successful in distinguishing the diverse sediment facies and their distribution throughout the lake. In the case of Lake Seracchi, we can state that the silty-clay sediment is spread in most of the lake, with the few exceptions of small areas near the inflow and some large rocks in two locations (Figures 4b, 6b, and 7). This means that the geotechnical properties of the fine sediment, investigated by laboratory analyses on manually collected samples, can be extrapolated, with caution, as representative of the whole area of the lake.

The interesting cases of two geotechnical properties, inferred in such a way—infiltration rate and friction angle—are detailed in the following two subsections.

5.4 | Infiltration rate

The grain-size distribution analysis allows estimating the hydraulic conductivity (k, measured in m/s) of the sediment layer, under the assumption, described in the above paragraph, that geotechnical parameters can be taken from a few sampling points and considered representative of areas covered by indirect geophysical surveys. Since the methodology also measures the hydraulic gradient (≈ average water depth) and the average sediment layer thickness, a rough estimation of the infiltration rate can be performed using Darcy's law (Darcy, 1856).

According to Equation (2), the sediments of Lake Seracchi have k of the order of 10^{-12} m/s. This result has to be taken qualitatively, because of the limited number of samples herein considered, and k depends on several variables of the texture structure, which can be described by a shape factor (Taylor, 1948). Nevertheless, Clarke pointed out that similar glacial flour, with fine particles > 35%, has hydraulic conductivity $k < 10^{-9}$ m/s (Clarke, 2018).

Considering a hydraulic gradient equal to 4 m, sediment layer thickness = 1.5 m, total area = 10^5 m^2, and $k = 10^{-12}$ m/s, the infiltration rate is practically inexistent. Even if, more conservatively, k is taken equal to 10^{-9}, the infiltration rate is about 2.7×10^{-4} m^3/s—three orders of magnitude lower than the water flow in the lake, estimated to be about 0.6 m^3/s in the summer months (Dr Elisabetta Corte, personal communication). Even if the order of magnitude of this result is mostly dependent on the rough estimation of k, it is reasonably certain that there is a negligible infiltration rate in Lake Seracchi.

We stress that the importance of integrating geophysical and geotechnical techniques relies on the fact that the estimation of the infiltration rate of the lake is possible only because the GPR and TDR measurements were able to survey almost all the lake area and detect spatial differences in the sediment properties. Since the silty-clay layer is observed to be present all over the lake, and with a consistent thickness, the hydraulic conductivity property—and therefore the infiltration rate—can be extrapolated with confidence to almost all the lake area, starting from just a few manually collected samples.

These considerations, applied to the specific case of Lake Seracchi, depict a situation different from that observed a century ago by Preller, as mentioned at the second point of his conclusions (Preller, 1918). He speculated that a great loss of water was ongoing through the very permeable moraines or glacial sediments of the Rutor basin terraces, while today, at least for the Lake Seracchi area, the thick sediment layer is almost impermeable.

5.5 | Friction angle

The liquid and plastic limits are properties that deal with the mechanical behavior of the material; thus they are pivotal in modeling failures, landslides, debris flows, or other risks typical of deglaciated areas or associated with GLOFs. As for the sediment layer hydraulic conductivity, also Atterberg's limits and the derived mechanical properties may be representative of the wider areas covered by the geophysical survey.

A valuable contribution by Wu and Kenney extensively discussed how to estimate the mechanical properties of clays from deposits found in areas formerly occupied by glacial lakes, focusing on both petrographic aspects and geotechnical indices (Kenney, 1959; Wu, 1958, 1960). The reported analyses deal with samples from multiple sites, mostly thick layers of silty-clays similar, for petrographic aspects and deposition processes, to those of Lake Seracchi. Particularly, they discussed empirical relationships to link different properties of glacial lake clays, such as the plasticity index, to very valuable strength properties, like friction angle. Their study focused on the fact that the features of sampled clays and tills depend on the lithology of the rock formation from which they come, the location in which they are transported along the glacier, and the mode of deposition. Lithology influences both grain-size distribution and density of glacial lake clays; whereas deposition processes in lakes and basins, such as the case of Lake Seracchi, generally produce over-consolidated sediment. In Figure 13 an empirical correlation between the plasticity index and the effective stress friction angle is presented. The two square symbols near PI = 10, collected by Kenney, show the friction angle of a glacial till sediment very similar to that of Lake Seracchi. Therefore, it is expected that the friction angle of Lake Seracchi sediment is about $\phi' = 35°$, intended as the effective shear strength angle; this value is quite high and, as Wu and Kenney suggest, arises from deposition modes, loading and unloading during freeze periods and mineralogic types present in the site.

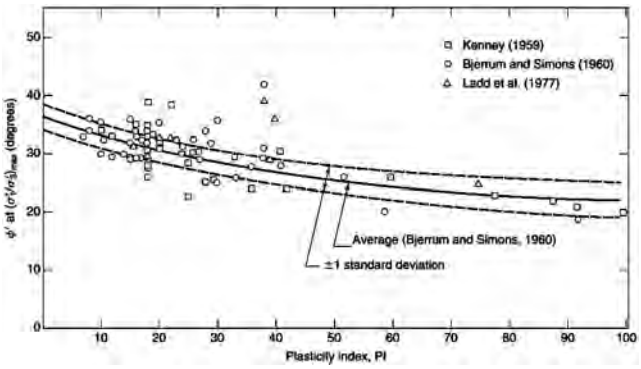

FIGURE 13 Empirical correlation between effective stress friction angle ϕ' (from triaxial compression tests on normally consolidated undisturbed clays) and plasticity index (after Holtz et al., 1981)

10969837, 0, Downloaded from https://onlinelibrary.wiley.com/doi/10.1002/esp.5555 by CochraneItalia, Wiley Online Library on [14/02/2023]. See the Terms and Conditions (https://onlinelibrary.wiley.com/terms-and-conditions) on Wiley Online Library for rules of use; OA articles are governed by the applicable Creative Commons License

5.6 | Sedimentation in Lake Seracchi

Several techniques were merged into one integrated methodology to assess the spatial distribution of numerous properties and characteristics of the test site. In the following we discuss the implications and contributions to the knowledge of Lake Seracchi, to give insights about the area useful for further local studies, and evaluate the quantity and quality of information that this methodology can provide when applied to other proglacial lakes.

Glacier flour is produced by the subglacial erosion of the Rutor glacier and sediments on the bottom of the lake, forming a thick impermeable layer (>1 m). This silty-clayish layer has geophysical and especially geoelectrical properties different from coarser sediments. Surveying those properties all over the lake allows us to deduce that this layer is distributed all over the lake, even if some exceptions are detected near the inflows and in the presence of larger rocks. The material has a high content in fines and, notwithstanding the apparent adhesion when pulling out the manual sampler, the measured plasticity is low, and also the liquid limit is low. Probably, the long time of compaction, and the load–unload cycles due to seasonal variations in water depth, positively favored a cohesive behavior rather than a plastic behavior.

The sediment distribution and the sediment volume (around 150.000 m^3) can bring interesting considerations, looking from a historical point of view: since its formation around 1880, Lake Seracchi accumulated more than 1000 m^3 of sediments per year on average, which corresponds to about 1 cm of added thickness every year. Note that this refers only to the very fine sediment—silty-clayish, the glacier flour—because also the deposition of coarser sediments was detected, near the inflows. A very rough prediction would indicate that in 100 years the areas of the lake shallower than 1 m will be filled by sediments, reshaping the lake (see Figure 4a) for the 1 m contour lines). However, the complex process of sedimentation could change rapidly in response to glacier shrinking and climate variations, and needs more data and research to be understood. For example, future research could involve: direct measurements of suspended solids content in various areas of the lake with a turbidimeter; finite-element modeling of water flow and sedimentation rate; studies on the quantity of suspended solids that will come from the subglacial erosion, considering the effects of shrinkage of the glacier, the opening of new deglaciated zones and the formation of new lakes (which are sediment sinks) in the upper proglacial areas of the Rutor basin.

In the last summer months, about 0.6 m^3/s of water flow in the lake was measured (Elisabetta Corte, personal communication), which corresponds to about 0.5 mm/s of average flow velocity in the lake. This is a very rough estimation based on a simplified geometry, not on a more developed finite element flow model, so there will be a difference based on the different zones of the lake. However, it can be used for a first perspective of the sedimentation rate using the Stokes equation:

$$v = \frac{2(\rho_p - \rho_f) r^2 g}{9\mu} = \frac{2 \times (2.5 - 1) \times \left(2 \times 10^{-6}\right)^2 \times 9.8}{9 \times 1.5 \times 10^{-3}} \cong 9 \times 10^{-9} \frac{m}{s}, \quad (3)$$

where the density of the particle is about 2.5 kg/m^3, its radius is taken as 2×10^{-6} m, as an average of the samples grain-size distribution, and μ is the viscosity of water at 6°C. This result means that, in about 300 m of horizontal water flow at 0.5 mm/s, there is an average submerging of a clay particle of about 5 mm, which is clearly not enough to reach the bottom of the lake (average = 3.9 m depth). According to this calculation, it can be supposed that only a small fraction of the suspended solids remains trapped in the lake, and the greater part continues its path downstream. This rough estimate, however, does not consider the possible aggregation of particles, which could increase their effective diameter and provide faster sedimentation; therefore, this topic should be further deepened for studies on solid transport flow. Certainly, sedimentation can occur in summer in zones of stagnation, and everywhere in winter, when the surface is frozen and the water flow stops. Future monitoring of turbidity in different areas of the lake could shed light on the question.

The sedimentation process near the inflow from the glacier represents another interesting chapter not investigated in this study, which would require sampling the southeast area of the lake. This area could be adequate for studying the seasonality of the sedimentation process, searching for varve stratification in the sediments, as performed in several studies (Karlén, 1981; Mihu-Pintilie et al., 2016; Németh et al., 2014; Zolitschka et al., 2015). In this sense, the test site is excellent because knowledge about its hydrogeological history is relatively extensive (and, being recent, it is possible to model the seasonal variations, and their causes, since its birth; Maussion et al., 2021).

Regarding, in particular, the inflow from Lake Santa Margherita, some insights can be obtained by comparing Figures A4 and A6 in Appendix A. The first was drawn in 1860 and the second in 1979, whereas the event that emptied Lake Santa Margherita occurred in 1864. During the flood, almost surely the Lake Seracchi area was still covered by ice and so no deposition could occur at that time. However, the progressive retreat of the glacier in those and following years exposed a deglaciated area in which material of different grain sizes could be abundant. We speculate that the newly formed channel connecting Lake Santa Margherita and the new Lake Seracchi (visible as a small pond in Figure A6) flowed through this deglaciated zone carrying material of various grain sizes (probably containing the gravel shown in Figure 12, plus some larger boulders and also finer sediments). In Figure A6 the deglaciated zone is referred to as "moraine."

5.7 | Past and future perspectives

Reading and analyzing the past history of a site is part of a correct approach or methodology, and some considerations are discussed in this subsection. Combining past information with the results of the measurements, some future perspectives on the application of the methodology, at Lake Seracchi or elsewhere, are suggested.

The history of the lake begins in about 1880, after the retreat of the Rutor glacier and the great shrinking of Lake Santa Margherita from the event of 1864. Lake Seracchi has been changing since its birth, as reported in Figures A1–A8, mostly due to the retreat of the Rutor glacier and to the solid transport from glacier runoff. Looking at the history of the Rutor basin, lakes have formed in the terraced morphology of the Rutor basin, due to the glacier retreat, in the positions of the previous glacier overdeepenings. The formation of new lakes will be due to the further shrinking of the glacier, predicted by all glacier–climate models (Carturan et al., 2020; Haeberli et al., 2019;

10969837, 0, Downloaded from https://onlinelibrary.wiley.com/doi/10.1002/esp.5555 by CochraneItalia, Wiley Online Library on [14/02/2023]. See the Terms and Conditions (https://onlinelibrary.wiley.com/terms-and-conditions) on Wiley Online Library for rules of use; OA articles are governed by the applicable Creative Commons License

Maussion et al., 2019; Oerlemans, 2005), and past research revealed where new lakes should be situated (Viani et al., 2020). Because of future changes, solid transport towards Lake Seracchi may also change, mainly for two reasons (Comiti et al., 2019; Lane et al., 2017). First, the glacier retreat can expose zones with soft subglacial sediments, which will be rapidly eroded by the water drainage system and carried into Lake Seracchi, increasing the solid transport towards it. Instead, a second ongoing phenomenon—the formation of new lakes in the upper basin that discharge water into Lake Seracchi (Viani et al., 2020)—will represent potential sediment sinks (Karlén, 1981). They will store the fine glacial flour coming from the glacier, releasing more transparent water into Lake Seracchi. The sedimentation process, which, in 140 years, accumulated about 150,000 m^3 of sediments, could be decreased or stopped. Also, the clearer waters will allow vegetation to develop, and the sediment layer should store this information because it would accumulate organic matter.

Future field measurements can contribute to a more comprehensive view of sediment distribution, its characteristics, and its temporal evolution. The water turbidity could be measured directly on site, in different zones of the lake, to better understand the solid transport and the sedimentation process. Temperature and turbidity of glacier meltwaters can be measured together, since they may vary considerably on seasonal and diurnal timescales, resulting in complex patterns of underflow, interflow, and overflow in glacier-fed lakes (Filella et al., 2009; Irwin & Pickrill, 1982). Joint measurements of flow rate and turbidity will make it possible to evaluate the sedimentation history of the lake, thanks to the map of the current sediment thickness produced in this paper. Measurements of the glacier activity, such as the mass balance and snow water equivalent (Godio & Rege, 2016), or glacier retreat modeling (Viani et al., 2020), can enhance the comprehension of the dependence of Lake Seracchi on the Rutor glacier. Repeating the GPR survey after some years can prove the increase in sediment thickness, as performed in a previous study (Mihu-Pintilie et al., 2016). In future research, it would be interesting also to study the seasonality of the sedimentation process in Lake Seracchi, due to variations of water depth during the year (see Figure 5) and winter freezing. Unfortunately, the main evidence to show seasonality in a lake sedimentation process—that is, the observation of varves, a term used to describe the stratification of a coarser and a finer sediment layer—was not observed in our samples. Probably, this is because both were collected very far from the main inflow from the glacier, so the coarser sediments could not reach those locations, even with the greater kinetic energy due to higher water flow during the summer. A sediment-sampling campaign near the inflow from the glacier would be welcomed to answer this research question. Other geotechnical properties interesting to investigate would be the undrained cohesion by vane test, the compaction by penetrometer tests, and the correlation between in situ and laboratory parameters. Also, evaluating the angle of contact will help in understanding the great cohesion of the sampled sediments—a property independent from the other mechanical parameters. The use of drones for investigating inaccessible proglacial lakes would also be an interesting research follow-up and the Rutor basin could be an adequate test site, due to the formation of new lakes in the upper part of the proglacial zone, with high and dangerous water flow, which discourages boat-based surveys.

A notable field of study for proglacial lakes is also regional-scale modeling, for which this methodology could be applied. Regional-scale studies about proglacial lakes do exist, such as Lehmann et al. (2018), which investigated the different colors of more than 1000 proglacial lakes in New Zealand from satellite imagery, to understand the time variations in glacier flour inflow. This and other models could be confirmed or enhanced by ground-based surveys such as the one presented in this paper. Those regional-scale studies (Rose et al., 2014), or comparative studies (Bogen et al., 2015), on sedimentation in proglacial lakes are important and valuable, but complex, and introduce several simplifications. This methodology has to be adapted to every specific site; for example, for the nearby Lake Santa Margherita the GPR results were not able to penetrate the whole layer of sediments. The main reason is that the factors influencing the sedimentation process are many: they span from the hydraulic characteristics of the lake to the petrography of the suspended solids; other factors are seasonality, sudden events, and anthropogenic impacts. All of these factors are strictly linked to the shrinkage of glaciers and the widening of the proglacial zone—strongly site-specific phenomena which depend on predictions based on an uncertain climate future.

6 | CONCLUSIONS

Lake Seracchi is a proglacial lake formed 140 years ago in an overdeepening of the retreating Rutor glacier. In July 2021, it had a depth of almost 11 m and an average depth of 3.9 m, covering an area of about 95,000 m^2. The subglacial erosion of the Rutor glacier was observed to produce silty-clayish glacier flour, which accumulated on the bottom of the lake, year after year, reaching an average thickness of 1.6 m, which was higher near the glacier inflows. We speculate that the future sediment transport in Lake Seracchi could change in the future mainly because of two interesting processes. On one hand, glacier retreat will expose soft sediments which will rapidly flow downstream, possibly increasing the sediment transport in the basin. On the other hand, the formation of new lakes in place of overdeepenings of the glacier upstream, compared to Lake Seracchi, could decrease the sediment carried to Lake Seracchi, because the new lakes will act as sediment sinks.

The methodology proposed was effective in identifying the fine sediment accumulated on the bottom of the test site—the proglacial Lake Seracchi—and evaluating its thickness and spatial distribution. Different kinds of sediment, with different granulometry, were identified by direct sampling and indirect geophysical surveys, using GPR and TDR. GPR managed to map the bathymetry of Lake Seracchi, providing a clear view of the water–bottom interface. Its main advantage, compared to other techniques, was the ability to detect also a second interface, useful to estimate the sediment layer thickness. TDR point measurements on the lake bottom estimated its electrical conductivity and dielectric permittivity, the latter being correlated with the electromagnetic wave velocity in the sediment. This was a necessary step to convert the GPR travel times to the actual sediment layer thickness. Jointly with the geophysical surveys, manual sampling was carried out and the main geotechnical properties were analyzed in the lab to determine grain-size distribution and Atterberg's limits. These are properties necessary to confirm the geophysical survey and to assess the sedimentation state of the lake and its past and future processes. The strength of the joint geotechnical–geophysical methodology is the capability to extend the geotechnical information, collected in a few points, to all those areas that share with the sampling points some

10969837, 0, Downloaded from https://onlinelibrary.wiley.com/doi/10.1002/esp.5555 by CochraneItalia, Wiley Online Library on [14/02/2023]. See the Terms and Conditions (https://onlinelibrary.wiley.com/terms-and-conditions) on Wiley Online Library for rules of use; OA articles are governed by the applicable Creative Commons License

key geophysical properties, such as electrical conductivity. This allows for faster and wider surveys, and also extends the applicability of proglacial lake sedimentation studies to remote areas difficult or onerous to sample. The Lake Seracchi study site was used to validate the proposed methodology and represented also a very interesting test site deserving of further study.

A limitation of the methodology, observed at the test site, is that GPR signal dispersion and attenuation at water depths greater than 6–7 m prevented detection of the sediment layer and, in those areas, the second interface was lost. To increase the investigation depth slightly, a lower-frequency antenna could be used—for example, 70 MHz—at the expense of resolution. Also, other geophysical techniques could be employed, such as electrical resistivity tomography or soundings that make use of mechanical and not electromagnetic waves, which could reach greater depths. Another limitation of the methodology may be the choice of sampling locations; for example, in the test survey, no samples were taken near the inflows from the glacier, and this limits the interpretation of the results. This kind of choice is strongly dependent on site and research objective. Possible extensions of the methodology mainly deal with the addition of direct measurements of solid transport flow or logistics-related innovations such as the use of drones.

This methodology is ready to be tested at other sites, but will require proper tuning in terms of geophysical instruments and choice of sampling locations, according to the specific conditions of the site and the goal of the research. Additionally, the dataset collected during the field test will enable future research to model the solid transport flow and predict the forthcoming changes in the interconnected landforms of the Rutor basin, as well as comparative studies with other proglacial lakes. The methodology could also help build regional-scale models, which need wide areas of ground-proof data.

CONFLICT OF INTEREST STATEMENT

The authors declare no conflict of interest.

ACKNOWLEDGEMENTS

The authors thank the following people: Dr Elisabetta Corte, for kindly providing the photos in Figures 2a and 2b and for the useful discussion about the history of the lake and the varve methodology; Dr Diego Franco, who helped with the instrument setup and the manual sampling of the sediments; the very gentle librarians of Museo della Montagna (Turin, Italy), for helping to retrieve the historical photos in Appendix A and part of the bibliography; Dr Paolo Maschio and Prof. Alberto Cina (Politecnico di Torino, DIATI Department), for kindly providing the high-resolution orthophoto in Figure 3; Dr Fabio Villa, for kindly permitting us to reproduce the map in Figure A8, and for the useful discussion about the Rutor glacier retreat; Dr Claudio de Regibus, for help in laboratory analysis and useful discussion about the nature of the sediments; Dr Melissa Latella, for her help during the GPR acquisition in Lake Santa Margherita; and two anonymous reviewers and the proofreaders, who greatly improved the quality of the manuscript. Open Access Funding provided by Politecnico di Torino within the CRUI-CARE Agreement.

FUNDING INFORMATION

This research was funded as one of the activities of the "CC-Glacier lab" of the MIUR project "Department of excellence" at the Politecnico di Torino—DIATI.

DATA AVAILABILITY STATEMENT

The data that support the findings of this study, in particular the bathymetry and sediment maps of Lake Seracchi, are available in the supplementary materials. The cited Zenodo repository contains also raw and processed GPR data: Vergnano A, Godio A, Oggeri C. Bathymetry and Sediment thickness distribution of Lago dei Seracchi alpine lake, Rutor basin, Aosta Valley, Italy. 2022. Dataset available at: 10.5281/zenodo.6021688.

ORCID

Andrea Vergnano https://orcid.org/0000-0001-9696-6747

REFERENCES

Al-Moadhen, M.M., Clarke, B.G. & Chen, X. (2020) The permeability of composite soils. *Environmental Geotechnics*, 7(7), 478–490. Available from: https://doi.org/10.1680/jenge.18.00030

Ameratunga, J., Sivakugan, N. & Das, B.M. (2016) Geotechnical Properties of Soils – Fundamentals. In: *Correlations of soil and rock properties in geotechnical engineering. Developments in geotechnical engineering*. New Delhi: Springer India, pp. 11–50. https://doi.org/10.1007/978-81-322-2629-1_2

Armando, E. & Charrier, G. (1985) The peat formation of the Rutor glacier (Aosta Valley). Results obtained by palynostratigraphic study of new peat outcrops near the glacier snout. *Geografia Fisica e Dinamica Quaternaria*, 8, 144–149.

Badino F. Holocene vegetation and climate variability as recorded in high-altitude mires (Western Italian Alps). 2016. Accessed December 16, 2021. https://www.semanticscholar.org/paper/Holocene-vegetation-and-climate-variability-as-in-Badino/e341c58648da4c5a1eaf81ebf1f8392506b9e7a7

Badino, F., Ravazzi, C., Vallè, F., Pini, R., Aceti, A., Brunetti, M. et al. (2018) 8800 years of high-altitude vegetation and climate history at the Rutor glacier forefield, Italian Alps. Evidence of middle Holocene timberline rise and glacier contraction. *Quaternary Science Reviews*, 185, 41–68. Available from: https://doi.org/10.1016/j.quascirev.2018.01.022

Baretti, M. (1880) Il Lago del Rutor (Alpi Graje settentrionali). *Bollettino del "Club Alpino Italiano"*, 14(41), 43–98.

Bjerrum, L. & Simons, N.E. (1960) Comparison of shear strength characteristics of normally consolidated clays. In: *Proceedings of the Research Conference on Shear Strength of Cohesive Soils held in University of Colorado, Boulder, Colorado*. New York: American Society of Civil Engineers, p. 1164.

Bogen, J., Xu, M. & Kennie, P. (2015) The impact of pro-glacial lakes on downstream sediment delivery in Norway. *Earth Surface Processes and Landforms*, 40(7), 942–952. Available from: https://doi.org/10.1002/esp.3669

Boulton, G.S. & Paul, M.A. (1976) The influence of genetic processes on some geotechnical properties of glacial tills. *Quarterly Journal of Engineering Geology & Hydrogeology*, 9(3), 159–194. Available from: https://doi.org/10.1144/GSL.QJEG.1976.009.03.03

Bradford, J.H., Johnson, C.R., Brosten, T., McNamara, J.P. & Gooseff, M.N. (2007) Imaging thermal stratigraphy in freshwater lakes using georadar. *Geophysical Research Letters*, 34(24), L24405. Available from: https://doi.org/10.1029/2007GL032488

Carrel, G. (1867) Le Lac du Rutor. *Bollettino del "Club Alpino Italiano"*, 2(10–11), 400–403.

Carturan, L., Rastner, P. & Paul, F. (2020) On the disequilibrium response and climate change vulnerability of the mass-balance glaciers in the Alps. *Journal of Glaciology*, 66(260), 1034–1050. Available from: https://doi.org/10.1017/jog.2020.71

Casagrande, A. (1932) Research on the Atterberg limits of soils. *Public Roads*, 13(8), 121–136.

Chapuis, R.P. & Aubertin, M. (2003) On the use of the Kozeny-carman equation to predict the hydraulic conductivity of soils. *Canadian Geotechnical Journal*, 40(3), 616–628. Available from: https://doi.org/10.1139/t03-013

10969837, 0, Downloaded from https://onlinelibrary.wiley.com/doi/10.1002/esp.5555 by CochraneItalia, Wiley Online Library on [14/02/2023]. See the Terms and Conditions (https://onlinelibrary.wiley.com/terms-and-conditions) on Wiley Online Library for rules of use; OA articles are governed by the applicable Creative Commons License

Clarke, B.G. (2018) The engineering properties of glacial tills. *Geotechnical Research*, 5(4), 262–277. Available from: https://doi.org/10.1680/jgere.18.00020

Colombo, G., Giaccone, E., Paro, L., Buffa, G. & Fratianni, S. (2016) The recent transition from glacial to periglacial environment in a high altitude alpine basin (Sabbione Basin, North-Western Italian Alps). Preliminary outcomes from a multidisciplinary approach. *Geografia Fisica e Dinamica Quaternaria*, 39(1), 21–36. Available from: https://doi.org/10.4461/GFDQ.2016.39.3

Comiti, F., Mao, L., Penna, D., Dell'Agnese, A., Engel, M., Rathburn, S. et al. (2019) Glacier melt runoff controls bedload transport in Alpine catchments. *Earth and Planetary Science Letters*, 520, 77–86. Available from: https://doi.org/10.1016/j.epsl.2019.05.031

D18 Committee. (2018) *Test methods for liquid limit, plastic limit, and plasticity index of soils*. West Conshohocken, PA, USA: ASTM International.

Darcy, H. (1856) *Les Fontaines Publiques de La Ville de Dijon: Exposition et Application Des Principes à Suivre et Des Formules à Employer Dans Les Questions de Distribution d'eau: Ouvrage Terminé Par Un Appendice Relatif Aux Fournitures d'eau de Plusieurs Villes, Au Filtrage Des Eaux et à La Fabrication Des Tuyaux de Fonte, de Plomb, de Tôle et de Bitume*. Paris: V. Dalmont. https://books.google.it/books?id=42EUAAAAQAAJ

Dreimanis, A. & Schlüchter, C. (1985) Field criteria for the recognition of till or tillite. *Palaeogeography Palaeoclimatology Palaeoecology*, 51(1–4), 7–14. Available from: https://doi.org/10.1016/0031-0182(85)90079-3

Favre, A. (1867) *Recherches Géologiques dans les Parties de la Savoie, du Piémont et de la Suisse voisines du Mont-Blanc. Avec un Atlas de 32 Planches*, Vol. 1. Paris: V. Masson et Fils. https://doi.org/10.1017/S0016756800207711

Filella, M., Chanudet, V., Philippo, S. & Quentel, F. (2009) Particle size and mineralogical composition of inorganic colloids in waters draining the adit of an abandoned mine, Goesdorf, Luxembourg. *Applied Geochemistry*, 24(1), 52–61. Available from: https://doi.org/10.1016/j.apgeochem.2008.11.010

French, H. & Harbor, J. (2013) 8.1 The Development and History of Glacial and Periglacial Geomorphology. In: *Treatise on geomorphology*. Amsterdam: Elsevier, pp. 1–18. https://doi.org/10.1016/B978-0-12-374739-6.00190-1

Gizzi, M., Mondani, M., Taddia, G., Suozzi, E. & Lo Russo, S. (2022) Aosta Valley Mountain Springs: A preliminary analysis for understanding variations in water resource availability under climate change. *Water*, 14(7), 1004. https://doi.org/10.3390/w14071004

Godio, A. & Rege, R.B. (2016) Analysis of georadar data to estimate the snow depth distribution. *Journal of Applied Geophysics*, 129, 92–100. Available from: https://doi.org/10.1016/j.jappgeo.2016.03.036

Gomez, C. & Miller, J. (2017. Accessed December 16, 2021) *Ground penetrating radar analysis of slope and Lake sediments interplay: A survey of Lake Pearson*. Kobe, Japan: Kobe University. https://hal.archives-ouvertes.fr/hal-01524351

Haeberli, W., Oerlemans, J. & Zemp, M. (2019) The Future of Alpine Glaciers and Beyond. In: *Oxford research encyclopedia of climate science*. Oxford, UK: Oxford University Press. https://doi.org/10.1093/acrefore/9780190228620.013.769.

Haldorsen, S. (1978) Glacial comminution of mineral grains. *Norsk Geologisk Tidsskrift*, 58(3), 241–243.

Haldorsen, S. (2008) Grain-size distribution of subglacial till and its reaction to glacial crushing and abrasion. *Boreas*, 10(1), 91–105. Available from: https://doi.org/10.1111/j.1502-3885.1981.tb00472.x

Heckmann, T., McColl, S. & Morche, D. (2016) Retreating ice: Research in pro-glacial areas matters: Research in pro-glacial areas. *Earth Surface Processes and Landforms*, 41(2), 271–276. Available from: https://doi.org/10.1002/esp.3858

Heckmann, T., Morche, D. & Becht, M. (2019) Introduction. In: Heckmann, T. & Morche, D. (Eds.) *Geomorphology of proglacial systems*, Geography of the physical environment. Cham, Switzerland: Springer International Publishing, pp. 1–19. https://doi.org/10.1007/978-3-319-94184-4_1.

Hill, N.E. (1970) The temperature dependence of the dielectric properties of water. *Journal of Physics C: Solid State Physics*, 3(1), 238–239. Available from: https://doi.org/10.1088/0022-3719/3/1/026

Holtz, R.D., Kovacs, W.D. & Sheahan, T.C. (1981) *An introduction to geotechnical engineering*, Vol. 733. Hoboken, NJ, USA: Prentice-Hall Englewood Cliffs.

Inman, D.L. (1949) Sorting of sediments in the light of fluid mechanics. *SEPM Journal of Sedimentary Research*, 19, pp. 51–70. Available from: https://doi.org/10.1306/D426934B-2B26-11D7-8648000102C1865D

Irwin, J. & Pickrill, R.A. (1982) Water temperature and turbidity in glacially fed Lake Tekapo. *New Zealand Journal of Marine and Freshwater Research*, 16(2), 189–200. Available from: https://doi.org/10.1080/00288330.1982.9515962

Karlén, W. (1981) Lacustrine sediment studies: A technique to obtain a continuous record of Holocene glacier variations. *Geografiska Annaler. Series a, Physical Geography*, 63(3–4), 273–281. Available from: https://doi.org/10.1080/04353676.1981.11880042

Kenney, T.C. (1959) Discussion of "geotechnical properties of glacial Lake clays". *Journal of the Soil Mechanics and Foundations Division*, 85(3), 67–79. Available from: https://doi.org/10.1061/JSFEAQ.0000201

Koenings, J.P. & Edmundson, J.A. (1991) Secchi disk and photometer estimates of light regimes in Alaskan lakes: Effects of yellow color and turbidity. *Limnology and Oceanography*, 36(1), 91–105. Available from: https://doi.org/10.4319/lo.1991.36.1.0091

Lachhab, A., Booterbaugh, A. & Beren, M. (2015) Bathymetry and sediment accumulation of Walker Lake, PA using two GPR antennas in a new integrated method. *Journal of Environmental and Engineering Geophysics*, 20(3), 245–255. Available from: https://doi.org/10.2113/JEEG20.3.245

Ladd, C.C., Foott, R., Ishihara, K., Schlosser, F. & Poulos, H.G. (1977) Stress-deformation and strength characteristics, state of the art report. In: *Proceedings of 9th ISFMFE*, Vol. 4. Tokyo: The Japanese Society of Soil Mechanics and Foundation Engineering, pp. 421–494.

Lane, S.N., Bakker, M., Gabbud, C., Micheletti, N. & Saugy, J.N. (2017) Sediment export, transient landscape response and catchment-scale connectivity following rapid climate warming and Alpine glacier recession. *Geomorphology*, 277, 210–227. Available from: https://doi.org/10.1016/j.geomorph.2016.02.015

Lehmann, M., Nguyen, U., Allan, M. & van der Woerd, H. (2018) Colour classification of 1486 lakes across a wide range of optical water types. *Remote Sensing*, 10(8), 1273. Available from: https://doi.org/10.3390/rs10081273

Linsbauer, A., Paul, F. & Haeberli, W. (2012) Modeling glacier thickness distribution and bed topography over entire mountain ranges with GlabTop: Application of a fast and robust approach: REGIONAL-SCALE MODELING OF GLACIER BEDS. *Journal of Geophysical Research - Earth Surface*, 117(F3), n/a–n/a. Available from: https://doi.org/10.1029/2011JF002313

Maussion, F., Butenko, A., Champollion, N., Dusch, M., Eis, J., Fourteau, K. et al. (2019) The open global glacier model (OGGM) v1.1. *Geoscientific Model Development*, 12(3), 909–931. Available from: https://doi.org/10.5194/gmd-12-909-2019

Maussion F, Rothenpieler T, Dusch M, Vlug A., Champollion N., Marzeion B. et al. (2021).*OGGM/OGGM: v1.5.2. Section: Hydrological mass-balance output*. Genéve, Switzerland: CERN. https://doi.org/10.5281/ZENODO.5327634

Mihu-Pintilie, A., Asandulesei, A., Nicu, I.C., Stoleriu, C.C. & Romanescu, G. (2016) Using GPR for assessing the volume of sediments from the largest natural dam lake of the eastern Carpathians: Cuejdel Lake, Romania. *Environment and Earth Science*, 75(8), 710. Available from: https://doi.org/10.1007/s12665-016-5537-1

Milner, A.M., Khamis, K., Battin, T.J., Brittain, J.E., Barrand, N.E., Füreder, L. et al. (2017) Glacier shrinkage driving global changes in downstream systems. *Proceedings of the National Academy of Sciences*, 114(37), 9770–9778. Available from: https://doi.org/10.1073/pnas.1619807114

Milton, C.J. (2018) Geophysics and geochemistry; an interdisciplinary approach to archaeology in wetland contexts. *Journal of Archaeological Science: Reports*, 18, 197–212. Available from: https://doi.org/10.1016/j.jasrep.2017.12.037

Monti, R. (1906) Recherches sur quelques lacs du Massif du Ruitor. *Annales de Biologie Lacustre*, 1, 120–167.

10969837, 0, Downloaded from https://onlinelibrary.wiley.com/doi/10.1002/esp.5555 by CochraneItalia, Wiley Online Library on [14/02/2023]. See the Terms and Conditions (https://onlinelibrary.wiley.com/terms-and-conditions) on Wiley Online Library for rules of use; OA articles are governed by the applicable Creative Commons License

Monti, R. (1929) Limnologia comparata dei laghi insubrici. *SIL Proc 1922–2010*, 4(1), 462–497. Available from: https://doi.org/10.1080/03680770.1929.11898422

Németh, A., Marcel, M., Grădinaru, I., Bihari, Á, Fekete, J. & Kern Z. (2014) *550 years in sedimentological record from a varved lake (Bolătău, Bukovina, NE Romania) – Changing storm frequency and climate fluctuation*. In GEOREVIEW: Scientific Annals of Stefan cel Mare University of Suceava. Geography Series. "Ştefan cel Mare". Vol. 24, no. 2. Romania: University Press, pp. 111–113. https://www.researchgate.net/publication/268817620_550_years_in_sedimentological_record_from_a_varved_lake_Bolatau_Bukovina_NE_Romania_-_changing_storm_frequency_and_climate_fluctuation

Nimbus, Società Metereologica Italiana. *Il ghiacciaio del Rutor ieri e oggi: ghiacci, acque e torbe*. 2012. Moncalieri (TO), Italy: Società Metereologica Italiana. Accessed December 17, 2021. http://www.nimbus.it/ghiacciai/2012/120927_Rutor.htm

Oerlemans, J. (2005) Extracting a climate signal from 169 glacier records. *Science*, 308(5722), 675–677. Available from: https://doi.org/10.1126/science.1107046

Orombelli, G. (2005) The Ruitor glacier (Aosta Valley) during the little ice age. *Geografia Fisica e Dinamica Quaternaria*. Published online, 7, 239–251.

Otto, J.C. (2019) Proglacial Lakes in High Mountain Environments. In: Heckmann, T. & Morche, D. (Eds.) *Geomorphology of proglacial systems. Geography of the physical environment*. Cham, Switzerland: Springer International Publishing, pp. 231–247. https://doi.org/10.1007/978-3-319-94184-4_14

Pelpola, C.P. & Hickin, E.J. (2004) Long-term bed load transport rate based on aerial-photo and ground penetrating radar surveys of fan-delta growth, Coast Mountains, British Columbia. *Geomorphology*, 57(3–4), 169–181. Available from: https://doi.org/10.1016/S0169-555X(03)00101-6

Preller, C.S.D.R. (1918) The Ruitor glacier lakes (Piedmontese Alps). *Scottish Geographical Magazine*, 34(9), 330–342. Available from: https://doi.org/10.1080/14702541808554167

Psarras, G.C. (2018) Fundamentals of Dielectric Theories. In: *Dielectric polymer materials for high-density energy storage*. Amsterdam: Elsevier, pp. 11–57. https://doi.org/10.1016/B978-0-12-813215-9.00002-6

Qi, Y. & Wu, Y. (2022) Electrical conductivity of clayey rocks and soils: A nonlinear model. *Geophysical Research Letters*, 49(10), e2021GL097408. Available from: https://doi.org/10.1029/2021GL097408

Qin, T., Zhao, Y., Shufan, H., An, C., Rao, C. & Geng, D. (2017). Profiling experiment of a lake using ground penetrating radar. In: *2017 9th international workshop on advanced ground penetrating radar (IWAGPR)*, Vol. 2017. New York, USA: IEEE, pp. 1–5. https://doi.org/10.1109/IWAGPR.2017.7996091

Rea JMA. *Ground penetrating radar applications in hydrology*. Vancouver, Canada: Ground penetrating radar applications in hydrology. University of British Columbia. Published online 1996. https://doi.org/10.14288/1.0052320

Regione Autonoma Valle d'Aosta. geoCartoSCT service. Accessed December 17, 2021. https://mappe.regione.vda.it/pub/geoCartoSCT/

rock flour|National Snow and Ice Data Center. Accessed February 1, 2022. https://nsidc.org/learn/cryosphere-glossary/rock-flour

Rose, K.C., Hamilton, D.P., Williamson, C.E., McBride, C.G., Fischer, J.M., Olson, M.H. et al. (2014) Light attenuation characteristics of glacially-fed lakes: Transparency of glacially-fed lakes. *Journal of Geophysical Research – Biogeosciences*, 119(7), 1446–1457. Available from: https://doi.org/10.1002/2014JG002674

Sacco, F. (1917) Il ghiacciaio ed i laghi del Ruitor. *Bollettino Della Societa Geologica Italiana*, 36(1), 1–36.

Sambuelli, L. & Bava, S. (2012) Case study: A GPR survey on a morainic lake in northern Italy for bathymetry, water volume and sediment characterization. *Journal of Applied Geophysics*, 81, 48–56. Available from: https://doi.org/10.1016/j.jappgeo.2011.09.016

Sambuelli, L., Calzoni, C. & Pesenti, M. (2009) Waterborne GPR survey for estimating bottom-sediment variability: A survey on the Po River, Turin, Italy. *Geophysics*, 74(4), B95–B102. Available from: https://doi.org/10.1190/1.3119262

Sambuelli L, Colombo N, Giardino M, Godone D. *A waterborne GPR survey to estimate fine sediments volume and find optimum Core location in a Rockglacier Lake*; presented at the Near Surface Geoscience 2015 - 21st European Meeting of Environmental and Engineering Geophysics, Turin, Italy, EAGE, Utrecht, Netherlands, 2015. https://doi.org/10.3997/2214-4609.201413826

Sambuelli, L., Comina, C., Bava, S. & Piatti, C. (2011) Magnetic, electrical, and GPR waterborne surveys of moraine deposits beneath a lake: A case history from Turin, Italy. *Geophysics*, 76(6), B213–B224. Available from: https://doi.org/10.1190/geo2011-0053.1

Sandmeier, K.J. (2012) *REFLEXW version 7.0-program for the processing of seismic, acoustic or electromagnetic reflection, refraction and transmission data. User's man*. Karlsruhe, Germany: Sandmeier, p. 578. https://www.sandmeier-geo.de/guides-and-videos.html

Schiefer, E. (2006) Contemporary sedimentation rates and depositional structures in a montane lake basin, southern Coast Mountains, British Columbia, Canada. *Earth Surface Processes and Landforms*, 31(10), 1311–1324. Available from: https://doi.org/10.1002/esp.1332

Shukla, S.B., Patidar, A.K. & Bhatt, N. (2008) Application of GPR in the study of shallow subsurface sedimentary architecture of Modwa spit, gulf of Kachchh. *Journal of Earth System Science*, 117(1), 33–40. Available from: https://doi.org/10.1007/s12040-008-0010-5

Sorensen, K. & Okkels, N. (2013) Correlation between drained shear strength and plasticity index of undisturbed overconsolidated clays. In: *Proceedings of the 18th international conference on soil mechanics and geotechnical engineering, Paris*, Vol. 1. London: ISSMGE, pp. 423–428.

Standard practice for classification of soils for engineering purposes (unified soil classification system). (n.d.). Accessed February 2, 2022. https://www.astm.org/d2487-17e01.html

Strigaro, D., Moretti, M., Mattavelli, M., Frigerio, I., Amicis, M.D. & Maggi, V. (2016) A GRASS GIS module to obtain an estimation of glacier behavior under climate change: A pilot study on Italian glacier. *Computational Geosciences*, 94, 68–76. Available from: https://doi.org/10.1016/j.cageo.2016.06.009

Tamburini, A. & Mortara, G. (2005) The case of the Effimero Lake at the Monte Rosa (Italian Western Alps): Studies, field surveys, monitoring. *IHP-VI Tech Doc Hydrology*, 77, 179–184.

Taylor, D.W. (1948) *Fundamentals of soil mechanics*. Hoboken, NJ, USA: J. Wiley.

Terzaghi, K., Peck, R.B. & Mesri, G. (1996) *Soil mechanics in engineering practice*, 3rd edition. Hoboken, NJ, USA: Wiley.

Tretjakova, R., Kodors, S., Soms, J. & Alksnis, A. (2019) CLAY DETECTION IN LAKES OF LATGALE USING GROUND PENETRATING RADAR. *Environment, Technologies, Resources. Proceedings of the International Scientific and Practical Conference*, 1, 291. Available from: https://doi.org/10.17770/etr2019vol1.4046

Vergnano, A., Franco, D. & Godio, A. (2022a) Drone-borne ground-penetrating radar for snow cover mapping. *Remote Sensing*, 14(7), 1763. Available from: https://doi.org/10.3390/rs14071763

Vergnano A, Godio A, Oggeri C. *Bathymetry and sediment thickness distribution of Lago Dei Seracchi alpine lake, Rutor basin, Aosta Valley, Italy*. 2022b. CERN, Genève, Switzerland, Dataset avaliable at: https://doi.org/10.5281/zenodo.6021688

Vergnano, A., Godio, A., Raffa, C.M., Chiampo, F., Bosco, F. & Ruffino, B. (2019) Time-domain reflectometry (TDR) monitoring at a lab Scale of aerobic biological processes in a soil contaminated by diesel oil. *Applied Sciences*, 9(24), 5487. Available from: https://doi.org/10.3390/app9245487

Viani, C., Machguth, H., Huggel, C., Godio, A., Franco, D., Perotti, L. et al. (2020) Potential future lakes from continued glacier shrinkage in the Aosta Valley region (Western Alps, Italy). *Geomorphology*, 355, 107068. Available from: https://doi.org/10.1016/j.geomorph.2020.107068

Villa, F., De Amicis, M. & Maggi, V. (2007) GIS analysis of Rutor glacier (Aosta Valley, Italy) volume and terminus variations. *Geografia Fisica e Dinamica Quaternaria*, 30(1), 87–95.

10969837, 0, Downloaded from https://onlinelibrary.wiley.com/doi/10.1002/esp.5555 by CochraneItalia, Wiley Online Library on [14/02/2023]. See the Terms and Conditions (https://onlinelibrary.wiley.com/terms-and-conditions) on Wiley Online Library for rules of use; OA articles are governed by the applicable Creative Commons License

Villa, F., Tamburini, A., Deamicis, M., Sironi, S., Maggi, V. & Rossi, G. (2008) Volume decrease of Rutor glacier (Western Italian Alps) since little ice age: A quantitative approach combining GPR, GPS and cartography. *Geogr Fis E Din Quat.*, 31(1), 63–70.

Ward, S.H. (Ed). (1990) *Geotechnical and environmental geophysics: Volume I: Review and tutorial*. Houston, TX, USA: Society of Exploration Geophysicists.

Wu, T.H. (1958) Geotechnical properties of glacial Lake clays. *Journal of the Soil Mechanics and Foundations Division*, 84, 1–34.

Wu, T.H. (1960) Closure to "Wu on glacial Lake clays". *Transactions of the American Society of Civil Engineers*, 125(1), 1021. Available from: https://doi.org/10.1061/TACEAT.0007924

Zolitschka, B., Francus, P., Ojala, A.E.K. & Schimmelmann, A. (2015) Varves in lake sediments – A review. *Quaternary Science Reviews*, 117, 1–41. Available from: https://doi.org/10.1016/j.quascirev.2015.03.019

SUPPORTING INFORMATION

Additional supporting information can be found online in the Supporting Information section at the end of this article.

How to cite this article: Vergnano, A., Oggeri, C. & Godio, A. (2023) Geophysical–geotechnical methodology for assessing the spatial distribution of glacio-lacustrine sediments: The case history of Lake Seracchi. *Earth Surface Processes and Landforms*, 1–24. Available from: https://doi.org/10.1002/esp.5555

10969837, 0, Downloaded from https://onlinelibrary.wiley.com/doi/10.1002/esp.5555 by CochraneItalia, Wiley Online Library on [14/02/2023]. See the Terms and Conditions (https://onlinelibrary.wiley.com/terms-and-conditions) on Wiley Online Library for rules of use; OA articles are governed by the applicable Creative Commons License

APPENDIX A

HISTORICAL CARTOGRAPHY AND PHOTOGRAPHY OF LAKE SERACCHI AND A PERSPECTIVE OF THE AUTHORS ABOUT ITS SEDIMENTATION HISTORY

In this appendix, we collected interesting (especially historical) material regarding the study site, with the hope of being useful for the interested reader.

Since the 1910s, the proglacial environment has attracted international interest from geoscientists after the definition of "periglacial zone" by Łozinzki (French & Harbor, 2013). However, scientific literature about proglacial areas dates back to an earlier time: since 1860, after the glacier retreat from the maximum extension of the LIA, such interest has grown, focusing especially on geology and biology, and sometimes the interest was driven by glaciological associations or local administrations (Baretti, 1880; Carrel, 1867; Monti, 1906). This is the case for the Rutor glacier basin and its proglacial lakes, which are very rich in historical documentation and cartography, reported in Figures A1–A8.

APPENDIX B.

OTHER SUPPORTING FIGURES AND TABLES

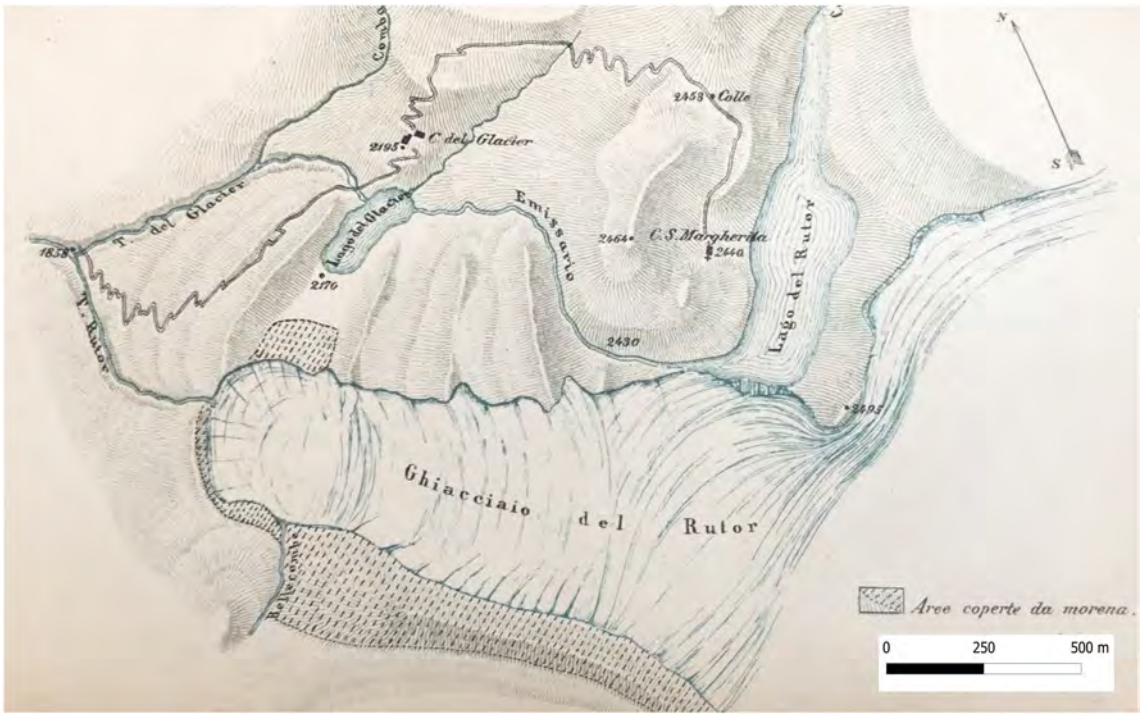

FIGURE A1 Chartography of Rutor basin in 1860 (Baretti, 1880). Lago del Rutor (= Lake Santa Margherita) fills the valley, blocked by the Rutor glacier, and discharges its water directly into Lac du Glacier, 250 m below. Lake Seracchi does not exist yet

FIGURE A2 Painting of Lake Santa Margherita in summer 1862 by Favre (1867). The current Lake Seracchi is completely covered by the thick ice of the Rutor glacier

10969837, 0, Downloaded from https://onlinelibrary.wiley.com/doi/10.1002/esp.5555 by CochraneItalia, Wiley Online Library on [14/02/2023]. See the Terms and Conditions (https://onlinelibrary.wiley.com/terms-and-conditions) on Wiley Online Library for rules of use; OA articles are governed by the applicable Creative Commons License

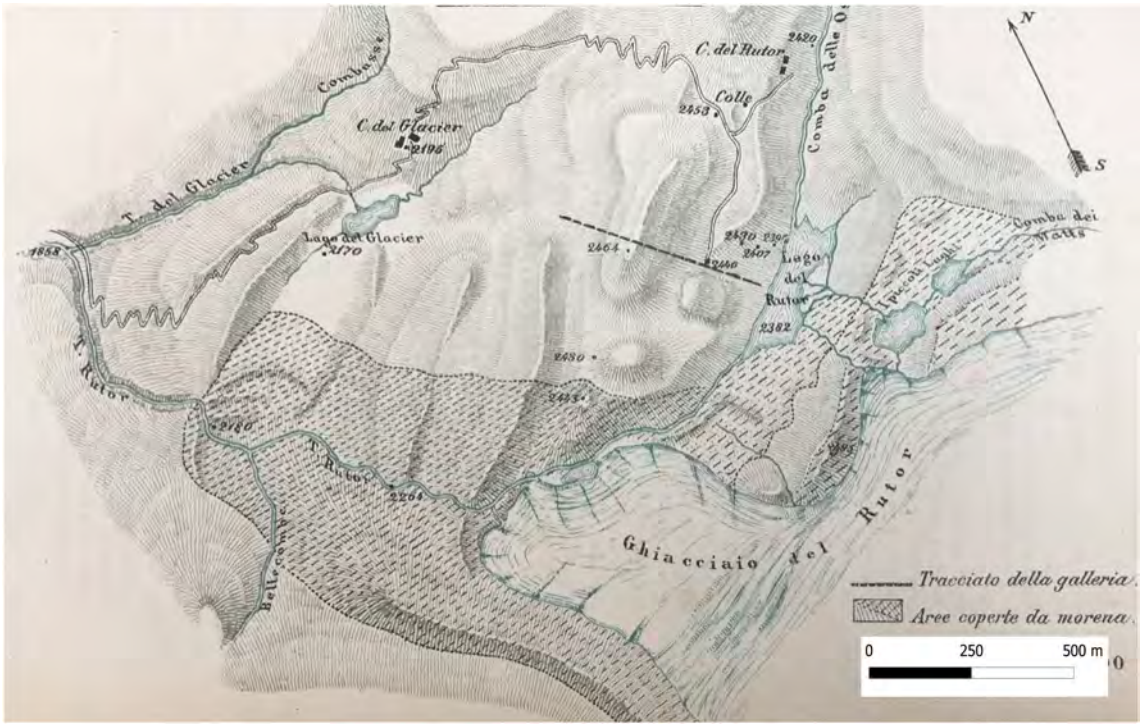

FIGURE A3 Chartography of Rutor basin in 1879 (Baretti, 1880). After the emptying of Lake Santa Margherita in 1864, the emissary flow completely changed its path, no longer going towards Lac du Glacier. A small pond, the future Lake Seracchi, begins to form at the glacier tongue

FIGURE A4 Photograph of Lake Seracchi (on the right side) in 1886 by Casanova (Sacco, 1917). Lake Seracchi occupies an area that nowadays is emerged (Sacco, 1917), and it is still mostly covered by ice. The marginal lake on the left is a small remaining of the old Lake Santa Margherita, still blocked by moraine and the glacier. The main part of Lake Santa Margherita is further upstream (not visible in the photo)

10969837, 0, Downloaded from https://onlinelibrary.wiley.com/doi/10.1002/esp.5555 by CochraneItalia, Wiley Online Library on [14/02/2023]. See the Terms and Conditions (https://onlinelibrary.wiley.com/terms-and-conditions) on Wiley Online Library for rules of use; OA articles are governed by the applicable Creative Commons License

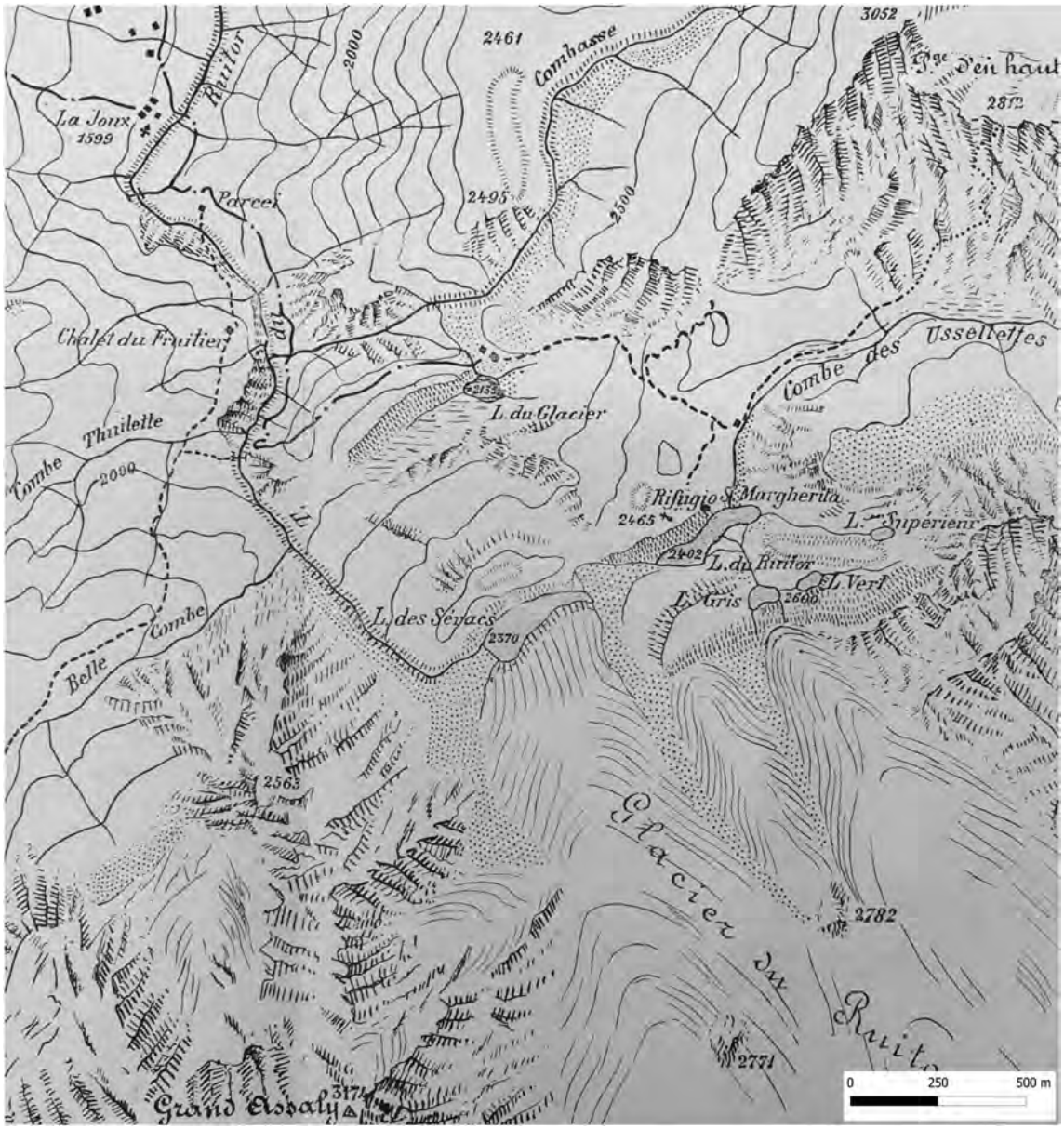

FIGURE A5 Chartography of Rutor basin in 1906 (Monti, 1906). Lake Seracchi (= L. des Séracs) is still directly connected to the lowest part of the Rutor glacier. Its ecosystem is not yet developed, except for simple bacteria, diatoms, and snow algae (Monti, 1929). (L. du Ruitor = Lake Santa Margherita)

10969837, 0, Downloaded from https://onlinelibrary.wiley.com/doi/10.1002/esp.5555 by CochraneItalia, Wiley Online Library on [14/02/2023]. See the Terms and Conditions (https://onlinelibrary.wiley.com/terms-and-conditions) on Wiley Online Library for rules of use; OA articles are governed by the applicable Creative Commons License

FIGURE A6 Photograph of Lake Seracchi (on the right side) in 1909 by Brocherel; it has a shape quite similar to the current one, but the Rutor glacier is still projecting into the lake (Sacco, 1917)

FIGURE A7 Chartography of Rutor basin in 1916 (Sacco, 1917). Lake Seracchi has a more familiar shape also in this map, but part of it is still covered by the glacier. By zooming in on the image, it is possible to explore Sacco's reconstruction of the area variations of Rutor glacier from 1820 to 1916

10969837, 0, Downloaded from https://onlinelibrary.wiley.com/doi/10.1002/esp.5555 by CochraneItalia, Wiley Online Library on [14/02/2023]. See the Terms and Conditions (https://onlinelibrary.wiley.com/terms-and-conditions) on Wiley Online Library for rules of use; OA articles are governed by the applicable Creative Commons License

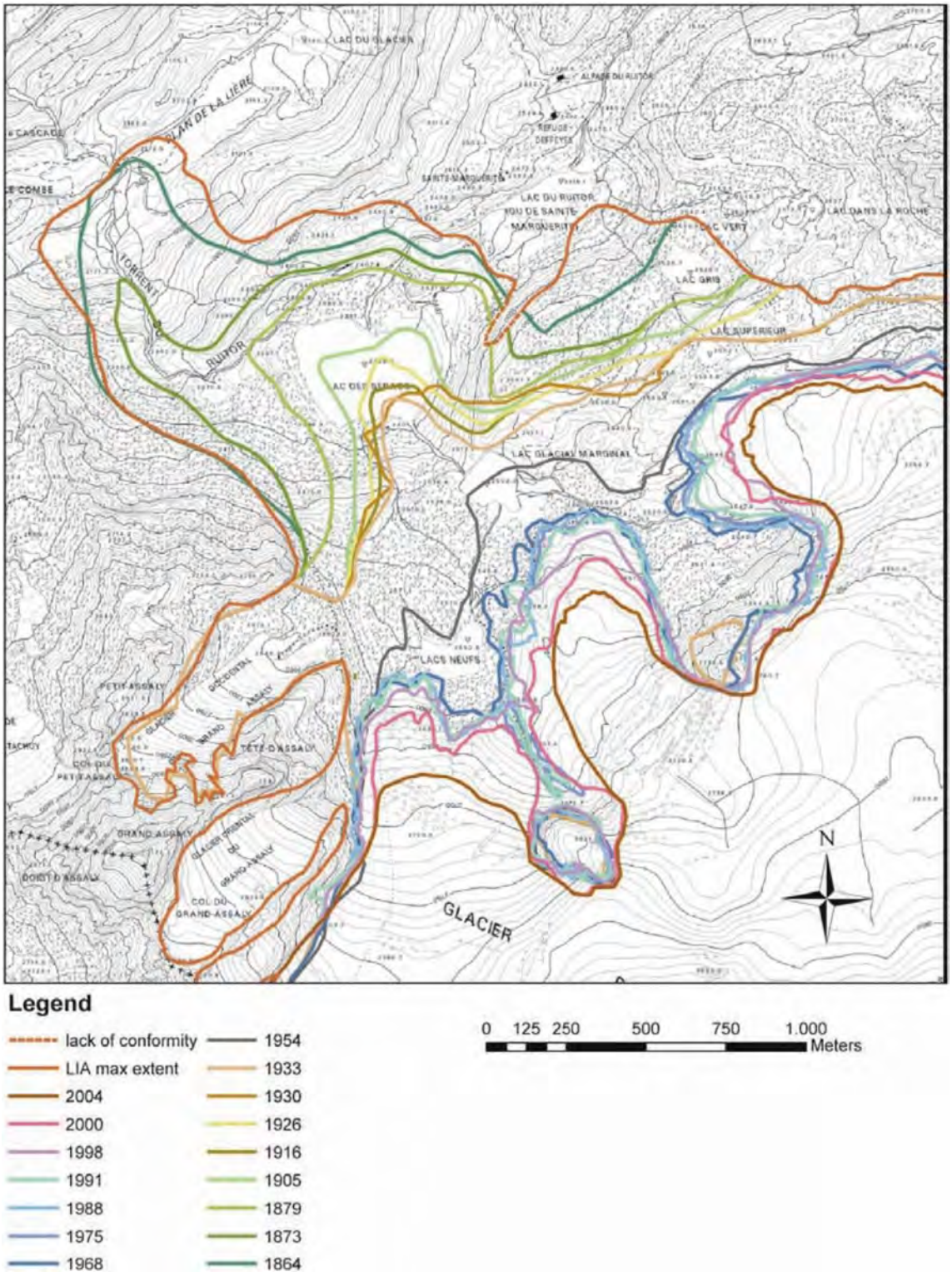

FIGURE A8 A recent reconstruction of the deglaciation process of Rutor glacier reveals the complete formation timeline of Lake Seracchi. In the center of the picture, "Lac Des Seracs" is the French name of Lake Seracchi. Adapted from Villa et al. (2007) with permission

10969837, 0, Downloaded from https://onlinelibrary.wiley.com/doi/10.1002/esp.5555 by CochraneItalia, Wiley Online Library on [14/02/2023]. See the Terms and Conditions (https://onlinelibrary.wiley.com/terms-and-conditions) on Wiley Online Library for rules of use; OA articles are governed by the applicable Creative Commons License

FIGURE B1 Aerial view of the glacier and proglacial zone. Photo by nimbus.it (September 15, 2012) (Nimbus, Società Metereologica Italiana, 2012)

FIGURE B2 The inflatable boat carrying the GPR system. All components are ruggedized and protected from water splashes

10969837, 0, Downloaded from https://onlinelibrary.wiley.com/doi/10.1002/esp.5555 by CochraneItalia, Wiley Online Library on [14/02/2023]. See the Terms and Conditions (https://onlinelibrary.wiley.com/terms-and-conditions) on Wiley Online Library for rules of use; OA articles are governed by the applicable Creative Commons License

TABLE B1 Results from TDR measurements. In red, the measurements on coarse sediment. In bold, a probable outlier due to measurement inaccuracies

Name	CMT	UTM_zone	UTM_east	UTM_north	Permittivity	Conductivity (S/m)
21	10-JUL-21 11:14:04	32	342591.8	5059269	37	0.0034
22	**10-JUL-21 11:15:25**	**32**	**342620**	**5059255**	**51**	**0.0034**
23	10-JUL-21 11:17:18	32	342657.9	5059261	41	0.0047
24	10-JUL-21 11:18:48	32	342684.6	5059258	39	0.0047
25	10-JUL-21 11:20:44	32	342704.8	5059250	39	0.0051
26	10-JUL-21 11:22:23	32	342733.2	5059249	41	0.0038
27	10-JUL-21 11:23:35	32	342735.9	5059218	38	0.0049
28	10-JUL-21 11:24:32	32	342756.2	5059207	38	0.0053
29	10-JUL-21 11:25:33	32	342742.7	5059239	38	0.005
30	10-JUL-21 11:27:41	32	342714.2	5059198	37	0.0047
31	10-JUL-21 11:28:51	32	342694.2	5059206	37	0.0051
33	10-JUL-21 11:33:46	32	342653	5059195	36	0.0042
34	10-JUL-21 11:35:21	32	342625.2	5059210	36	0.0047
37	10-JUL-21 11:40:07	32	342631.7	5059159	33	0.0035
38	10-JUL-21 11:41:07	32	342,644	5059137	33	0.0037
40	10-JUL-21 11:44:56	32	342730.7	5059153	34	0.0042
41	10-JUL-21 11:46:39	32	342723.1	5059114	35	0.005
42	10-JUL-21 11:47:49	32	342706.6	5059116	33	0.0025
43	10-JUL-21 11:49:22	32	342693.3	5059112	30	0.0019
44	10-JUL-21 11:49:59	32	342689	5059112	33	0.0051
46	10-JUL-21 11:55:17	32	342635.8	5059102	29	0.0033
47	10-JUL-21 11:56:40	32	342607.4	5059085	29	0.002
48	10-JUL-21 11:57:43	32	342597.5	5059098	32	0.0015
49	10-JUL-21 11:59:52	32	342587.3	5059073	31	0.0045
50	29-OCT-21	32	342385.6	5059292	34	0.0045
51	29-OCT-21	32	342351.9	5059285	34	0.0041
52	29-OCT-21	32	342543	5059281	25	0.001
53	29-OCT-21	32	342537.8	5059267	28	0.0035

10969837, 0, Downloaded from https://onlinelibrary.wiley.com/doi/10.1002/esp.5555 by CochraneItalia, Wiley Online Library on [14/02/2023]. See the Terms and Conditions (https://onlinelibrary.wiley.com/terms-and-conditions) on Wiley Online Library for rules of use; OA articles are governed by the applicable Creative Commons License